CAPITAL UNIVERSITY OF SCIENCE AND TECHNOLOGY, ISLAMABAD

An Unsteady Magnetohydrodynamics Carreau Fluid Flow

by

Azra Bano

A thesis submitted in partial fulfillment for the
degree of Master of Philosophy

in the
Faculty of Computing
Department of Mathematics

2019

Copyright © 2019 by Azra Bano

I dedicate my dissertation work to my family and friends . A special feeling of gratitude to my loving parents and my late Uncle Essa Khan who have supported me all the since the beginning of my studies.

CERTIFICATE OF APPROVAL

An Unsteady Magnetohydrodynamics Carreau Fluid Flow

by

Azra Bano

(MMT171020)

THESIS EXAMINING COMMITTEE

S. No.	Examiner	Name	Organization
(a)	External Examiner	Dr. Amer Rasheed	LUMS, Lahore
(b)	Internal Examiner	Dr. Muhammad Afzal	CUST, Islamabad
(c)	Supervisor	Dr. Muhammad Sagheer	CUST, Islamabad

_____

Dr. Muhammad Sagheer

Thesis Supervisor

October, 2019

_____   _____

Dr. Muhammad Sagheer   Dr. Muhammad Abdul Qadir

Head   Dean

Dept. of Mathematics   Faculty of Computing

October, 2019   October, 2019

Author's Declaration

I, **Azra Bano** hereby state that my M.Phil thesis titled "**An Unsteady Magnetohydrodynamics Carreau Fluid Flow**" is my own work and has not been submitted previously by me for taking any degree from Capital University of Science and Technology, Islamabad or anywhere else in the country/abroad.

At any time if my statement is found to be incorrect even after my graduation, the University has the right to withdraw my M.Phil Degree.

(Azra Bano)

Registration No: MMT171020

Plagiarism Undertaking

I solemnly declare that research work presented in this thesis titled "**An Unsteady Magnetohydrodynamics Carreau Fluid Flow**" is solely my research work with no significant contribution from any other person. Small contribution/help wherever taken has been dully acknowledged and that complete thesis has been written by me.

I understand the zero tolerance policy of the HEC and Capital University of Science and Technology towards plagiarism. Therefore, I as an author of the above titled thesis declare that no portion of my thesis has been plagiarized and any material used as reference is properly referred/cited.

I undertake that if I am found guilty of any formal plagiarism in the above titled thesis even after award of M.Phil Degree, the University reserves the right to withdraw/revoke my MS degree and that HEC and the University have the right to publish my name on the HEC/University website on which names of students are placed who submitted plagiarized work.

(Azra Bano)

Registration No: MMT171020

Acknowledgements

All the praises and thanks to Almighty **Allah**; the Lord and the Creator of all creations by whom power and glory of all things are accomplished. I would like to give the credit of this thesis to my supervisor **Dr. Muhammad Sagheer**, Head of the mathematics department at Capital University of Science and Technology, Islamabad. His leadership and words of encouragement perk up my performance throughout the session. I am grateful for his mentorship. Thank you sir! Also a special thanks to my teacher **Dr. Shafqat Hussian** and all faculty members who provided constructive and amiable environment during the studies.

I would like to convey special thanks to my family members for their support and guidance. I would also take this opportunity to thanks my friends and students of mathematics department, who help me and corrected my mistakes during research.

(Azra Bano)

Registration No: MMT171020

Abstract

A numerical evaluation of the crucial physical properties of a 3D unsteady MHD flow along stretching sheet for a Carreau fluid in the presence of Hall current and radiation has been carried out. Further, the effects of Weissenberg number and power-law index have also been discussed. Meanwhile, by applying similarity transformations the nonlinear PDEs are transformed into system of ODEs. Furthermore the numerical solution of nonlinear ODEs, the shooting method has been used. The obtained numerical results are computed with the help of MAT-LAB. The tables and graphs describe the numerical results for different physical parameters which affect the velocity and temperature profiles.

Contents

List of Figures

List of Tables

Abbreviations

MHD   Magnetohydrodynamics

ODEs   Ordinary Differential Equations

PDEs   Partial Differential Equations

SQLM   Spectral Quasi-linearization Method

Symbols

u, v, w	Velocity component in x, y and z directions
T	Temperature of the fluid
α^*	Rosseland mean absorption coefficient
α_m	Thermal diffusivity of the fluid
β	Casson fluid parameter
η	Dimensionless similarity variable
γ	Constant
ν	Kinematic viscosity of the fluid
ρ	Density of the fluid
σ	Electrical conductivity of the fluid
σ^*	Stefan-Boltzmann constant
τ_{wx}	Shear stress component in x direction
τ_{wz}	Shear stress component in z direction
θ	Dimensionless fluid temperature
a	Constant
A	Unsteadiness parameter
$B(t)$	Time-dependent magnetic field
C_{fx}	Skin friction coefficient in x direction
C_{fz}	Skin friction coefficient in z direction
c_ρ	Specific heat capacity at constant pressure
f', g	Dimensionless velocity in x and z direction
κ	Thermal conductivity of the fluid
m	Hall current parameter

M	Magnetic parameter
N_r	Radiation parameter
Nu_x	Local Nusselt number
P_r	Prandtl number
q_w	Wall heat transfer coefficient
Re_x	Local Reynolds number
t	Time variable
T_∞	Fluid temperature at infinity
T_w	Fluid temperature at the surface
tr	Temperature ratio parameter
W_e	Weissenberg number
n	Power law-index
Γ	Time constant
$u_w(x,t)$	Time dependent stretching velocity
x, y, z	Space variable

Chapter 1

Introduction

During the past few decades, the boundary layer problems related to a stretching surface have attracted an extensive attention of researchers, because the number of applications related to this area are found in engineering and industrial manufacturing process. Actually the boundary layer has a meaningful concept in physics and fluid mechanics, which is introduced as the layer of the fluid in the region of a bounded area where the effects of viscosity are powerful. Moreover it is also a region in the flow field in which the fluid deforms with a relative velocity. Each primary fluid has some basic important properties which play an essential role in its dynamics. The stretching and cooling rates both are significant in manufacturing process for the effective results of the final product. A speedy change in stretching demages the final product because of sudden solidification, so it is essential to maintain the stretching rate. The 2D flow of an incompressible liquid within the boundary layer along the stretching surface was first presented by Crane [1]. Various researchers have studied the interesting fluid flow along a stretching sheet [2–5].

Magnetohydrodynamics (MHD) is a combination of three words, magneto means magnetic filed, hydro means water and dynamics means movements. Meanwhile the hydromagnetic flow is the analysis of magnetic properties of eletrically conducting fluid. Plasmas, liquid metals, salt water, and electrolytes are considered as magneto fluids. MHD flow has a wide range of applications in engineering

devices such as the design of heat exchanges, blood pumping machines and the MHD electric power generators. The main role of magnetic parameter in flow field produces a resistive force which maintains the flow and detains the boundary layer separation. A number of researchers, investigated the flow models which contains the hydromagnetic effects. On top of that, Pavlov [6] exmained the MHD flow of visous fluids along a stretching sheet. Alfven [7] established the existence of electromagnetic-hydro-dynamic waves. Sarpakaya [8] studied the flow of specific types of fluids in magnetic field.

The time-dependent flows are consider as unsteady flow. Wang [9] investigated the time dependent flow problems. Furthermore various researchers considered the impacts of induced magnetic field on the time dependent MHD flow within the boundary layer region [10–12]. Ishak et al. [13] studied the heat tranfer of a time dependent flow. The temperature variation between the surrounding and the ambient fluid, produce the radiation. The impact of Hall current on the time denpendent flow of heat was analyzed by Aziz [14]. Further, many other authors have investigated the effects of radiative parameter [15–17]. Pal [18] analyzed the impacts of Hall current and hydromagnetic on the unsteady flow.

The complicated behavior of stress-strain can be found in a type of fluids which is called non-Newtonian fluids. Moreover the non-Newtonian fluids have earned a considerable attention because a number of applications of these fluids are found in engineering and industry. The Casson fluid is one of the most important non-Newtonian fluids, which is used in metallurgy, food processing etc. Casson [19] introduced Casson fluid model for the pigment-oil suspensions. Casson fluid exhibits the properties of yield stresses. Whenever the shear stress is greater than the yield stress, the fluid acts like a liquid. Likewise, if shear stress is less than the yield stress the fluid acts like a solid. In the category of Casson fluids, Jelly, shampoo, toothpast, ketchup, tomato sauce, honey, soup and juices are founded. Actually, yield stress analysis is important for all complex structured fluids. Dash et al. [20] examined the Casson fluid inside a pipe containing a porous medium

homogeneously. Later on Eldabe et al. [21] investigated hydromagnetic flow of a Casson fluid bounded between two cylinders in rotating position. In addition, the magnetohydrodynamics flow of 3D Casson fluid with stretching sheet were presented and elaborated in the literature [22–24]. Recently, several authors investigated the Casson fluid with different parameters which have been discussed in the upcoming discussion. Ashraf et al. [25] studied the impacts of Hall current on the Casson fluid. A 3D unsteady flow of the Casson fluid along a stretching surface was studied by Butt et al. [26]. Homogeneous-heterogeneous reactions of Casson fluid was examined by Khan et al. [27]. Later on, several researchers worked on free convective electromagnetic flow of Casson fluid in virous conditions [28–31]. Maleque [32] investigated the MHD flow of Casson liquid along a rotating disk. Kataria and Patel [33] considered the ramped wall temperature with heat and mass transfer in hydromagnetic flow of Casson liquid through porous medium. The MHD Casson fluid with the effects of Hall, Dufour and thermal radiation was analyzed by Vijayaragavan and Karthikeyan [34]. The impacts of Hall and radiation on the unsteady Casson fluid flow was analyzed by Prashu and Nandkeolyar [35]. Additionally the combination of Newtonian fluid and power law model produces a non-Newtonian Carreau fluid. Actually the Carreau fluid is a special form of Newtonian fluids in which the viscosity effects depends upon the high and low shear rate. Due to diverse applications of Carreau model in industry and engineering, many researchers have worked on properties of such types of model. Hayat et al.[36] illustrated the flow properties of Carreau fluid along a stretching sheet. Moreover, various researchers have been investigating the Carreau fluid model for different flow problems [37–39]

1.1 Thesis Contributions

The present survey is focused on the numerical analysis of time dependent 3D magnetohydrodynamics flow of the Carreau fluid with the impacts of Hall and radiation. The proposed nonlinear PDEs are converted into system of ODEs by applying similarity transformations. Further, for finding the numerical results

of highly nonlinear ODEs, shooting method is utilized. The obtained numerical results are computed with the help of MATLAB. The impact of significant parameters on velocity profile along x and z direction and temperature profile, skin friction and Nusselt number have been discussed in graphs and tables.

1.2   Outline of Thesis

This research work is further classified into four main chapters.

Chapter 2 consist of some basic definitions, useful concepts and governing equations of the fluid which are needed for the upcoming chapters.

Chapter 3 contains the review work of Prashu and Nandkeolyar [35].

Chapter 4 concentrates on the analysis of an extension of [35].

Chapter 5 contains the summary of the entire study.

Chapter 2

Basic Definitions and Governing Equations

2.1 Basic Definitions

This chapter contains some basic definitions, basic laws and terminologies of the fluids, which would be used in the upcoming chapters.

Definition 2.1.1. (Fluid) [40]

"Fluids are substances whose molecular structure offers no resistance to external shear forces: even the smallest force causes deformation of fluid particles. Although a significant distinction exists between liquids and gases, both types of fluids obey the same laws of motion. In most cases of interest, a fluid can be regarded as continuum, i.e a continuous substance."

Definition 2.1.2. (Fluid Mechanics) [41]

"Fluid mechanics is defined as the science that deals with the behavior of fluids at rest (fluid statics) or in motion (fluid dynamics), and the interaction of fluids with solids or other fluids at the boundaries."

Definition 2.1.3. (Fluid Dynamics) [42]

"It is the study of the motion of liquids, gases and plasma from one place to

another. Fluid dynamics has a wide range of applications like calculating force and moments on aircraft, mass flow rate of petroleum passing through pipelines, prediction of weather, etc."

Definition 2.1.4. (Viscosity) [43]

"Viscosity is a quantitative measure of a fluid's resistance to flow. More specifically, it determines the fluid strain rate that is generated by a given applied shear stress. We can easily move through air, which has very low viscosity. Movement is more difficult in water, which has 50 times higher viscosity. Still more resistance is found in SAE 30 oil, which is 300 times more viscous than water. Try to slide your hand through glycerin, which is five times more viscous than SAE 30 oil, or blackstrap molasses. Fluids may have a vast range of viscosities. Mathematically it can be written as

$$\mu = \frac{\tau}{\dfrac{\partial u}{\partial y}}$$

where μ is viscosity coefficient, τ is shear stress and $\dfrac{\partial u}{\partial y}$ represents the velocity gradient or rate of shear strain. Therefore μ has dimensions of stress-time: $[\frac{FT}{L^2}]$ or $[\frac{M}{(LT)}]$."

Definition 2.1.5. (Kinematic Viscosity) [44]

"It is defined as the ratio between the dynamic viscosity and density of fluid. It is denoted by the Greek symbol ν, thus mathematically,

$$\nu = \frac{viscosity}{density} = \frac{\mu}{\rho},$$

where the unit of kinematic viscosity is $\dfrac{L^2}{T}$."

Definition 2.1.6. (Ideal Fluid) [44]

"A fluid which is incompressible and is having no viscosity, is known as an ideal fluid. An ideal fluid is only an imaginary fluid as all the fluids, which exist have some viscosity."

Definition 2.1.7. (Real Fluid) [44]

"A fluid which possesses viscosity, is known as real fluid. All the fluids, in actual practice, are real fluids."

Definition 2.1.8. (Newtonian Fluid) [44]

"A real fluid, in which shear stress is directly, proportional to the rate of shear strain (or velocity gradient), is known as a Newtonian fluid."

Definition 2.1.9. (Non-Newtonian Fluid) [44]

"A real fluid, in which the shear stress is not proportional to the rate of shear strain (or velocity gradient), is known as a Non-Newtonian fluid."

Definition 2.1.10. (Ideal Plastic Fluid) [44]

"A real fluid, in which shear stress is more than the yield value and shear stress is proportional to the rate of shear strain (or velocity gradient), is known as an ideal plastic fluid."

Definition 2.1.11. (Megnetohydrodynamics) [45]

"Magnetohydrodynamics (MHD) is concerned with the flow of electrically conducting fluids in the presence of magnetic fields, either externally applied or generated within the fluid by inductive action."

2.2 Properties of Fluid

Definition 2.2.1. (Heat Transfer) [46]

"Due to temperature difference, energy transfer is called heat transfer. Heat transfer occurs through different mechanisms."

Definition 2.2.2. (Conduction) [46]

"Due to collision of molecules in the contact form, heat is transferred from one object to another object this phenomenon is called conduction. Such types of heat transfer occurs in the solids."

Definition 2.2.3. (Radiation) [46]

"In the radiation process, heat is transferred through electromagnetic rays and

waves. It takes place in liquids and gasses. An example of radiation would be atmosphere, the atmosphere is heated by the radiation of the sun."

Definition 2.2.4. (Thermal Conductivity) [46]

"It is the property of a substance which measures the ability to transfer heat. Fourier's law of conduction which relates the flow rate of heat by conduction to the temperature gradient is

$$\frac{dQ}{dt} = -kA\frac{dT}{dx},$$

where A, k, $\frac{dQ}{dt}$ and $\frac{dT}{dx}$ are the area, the thermal conductivity, the temperature and the rate of heat transfer, respectively. The SI unit of thermal conductivity is $\frac{kgm}{s^3}$ and and the dimension of thermal conductivity is $[\frac{ML}{T^3}]$."

Definition 2.2.5. (Thermal Diffusivity) [46]

" The ratio of the unsteady heat conduction , of a substance to the product of specific heat capacity C_p and density ρ is called thermal diffusivity. It quantify the ability of a substance to transfer heat rather to store it. Mathematically, it can be written as

$$\alpha = \frac{\kappa}{\rho C_p}.$$

The unit and dimension of thermal Diffusivity in SI system are $m^2 s^- 1 and [LT^- 1]$ respectively."

2.3   Types of Flow

Definition 2.3.1. (Compressible and Incompressilble) [41]

"A flow is classified as being compressible or incompressible, depending on the level of variation of density during flow. Incompressibility is an approximation, and a flow is said to be incompressible if the density remains nearly constant throughout.

Therefore, the volume of every portion of fluid remains unchanged over the course of its motion when the flow (or the fluid) is incompressible. The densities of liquids are essentially constant, and thus the flow of liquids is typically incompressible. Therefore, liquids are usually referred to as incompressible substances. A pressure of 210 atm, for example, causes the density of liquid water at 1 atm to change by just 1 percent. Gases, on the other hand, are highly compressible. A pressure change of just 0.01 atm, for example, causes a change of 1 percent in the density of atmospheric air."

Definition 2.3.2. (Steady versus Unsteady) [41]
"The terms steady and uniform are used frequently in engineering, and thus it is important to have a clear understanding of their meanings. The term steady implies no change at a point with time. The opposite of steady is unsteady. The term uniform implies no change with location over a specified region. These meanings are consistent with their everyday use (steady friend, uniform distribution, etc.). The terms unsteady and transient are often used interchangeably, but these terms are not synonyms. In fluid mechanics, unsteady is the most general term that applies to any flow that is not steady, but transient is typically used for developing flows. When a rocket engine is fired up, for example, there are transient effects (the pressure builds up inside the rocket engine, the flow accelerates, etc.) until the engine settles down and operates steadily. The term periodic refers to the kind of unsteady flow in which the flow oscillates about a steady mean."

Definition 2.3.3. ((Viscous and Inviscid Flow) [41]
"When two fluid layers move relative to each other, a friction force develops between them and the slower layer tries to slow down the faster layer. This internal resistance to flow is quantified by the fluid property viscosity, which is a measure of internal stickiness of the fluid. Viscosity is caused by cohesive forces between the molecules in liquids and by molecular collisions in gases. There is no fluid with zero viscosity, and thus all fluid flows involve viscous effects to some degree. Flows in which the frictional effects are significant are called viscous flows. However, in many flows of practical interest, there are regions (typically regions not close to solid surfaces) where viscous forces are negligibly small compared to inertial or

pressure forces. Neglecting the viscous terms in such inviscid flow regions greatly simplifies the analysis without much loss in accuracy."

2.4   Conservation Laws

Definition 2.4.1. (Equation of Mass) [47]

"For any fluid, conservation of mass is expressed by the scalar equation

$$\frac{\partial}{\partial t}(\rho)_1 + \nabla.[(\rho)_1\mathbf{u}]$$

$$\Rightarrow \quad \frac{\partial \rho}{\partial t} + \nabla.(\rho\mathbf{u}) = 0. \tag{2.1}$$

Hence, a velocity profile represents an admissible (real) flow, if and only if it satisfies the continuity equation. For incompressible fluids, Equation (2.1) reduces to

$$\nabla.\mathbf{u} = 0, \tag{2.2}$$

where $\mathbf{u}$ is a velocity vector."

Definition 2.4.2. (Equation of Momentum) [47]

"For any fluid the momentum equation is

$$\frac{\partial}{\partial t}(\rho\mathbf{u}) + \nabla.[(\rho\mathbf{u})\mathbf{u}] - \nabla.T - \rho\mathbf{g} = 0. \tag{2.3}$$

Since $\mathbf{T} = -p\mathbf{I} + \tau$, the momentum equation take the form

$$\rho\left(\frac{\partial \mathbf{u}}{\partial t} + \mathbf{u}.\nabla\mathbf{u}\right) = \nabla.(\mathbf{T} = -p\mathbf{I} + \tau) + \rho\mathbf{g}. \tag{2.4}$$

Equation (2.3) is a vector equation and can be decomposed further into three scalar components by taking the scalar product with the basis vectors of an appropriate orthogonal coordinate system. By setting $\mathbf{g} = g\nabla z$, where z is the distance from an arbitrary reference elevation in the direction of gravity, Equation (2.3) can also

be expressed as

$$\rho \frac{D\mathbf{u}}{Dt} = \rho \left(\frac{\partial \mathbf{u}}{\partial t} + \mathbf{u}.\nabla \mathbf{u} \right) = \nabla.(\mathbf{T} = -p\mathbf{I} + \tau) + \rho(g\nabla z), \qquad (2.5)$$

where $\frac{D}{Dt}$ t is the substantial derivative. The momentum equation then states that the acceleration of a particle following the motion is the result of a net force, expressed by the gradient of pressure, viscous and gravity forces."

Definition 2.4.3. (Law of Conservation of Energy) [47]

"Conservation of thermal energy is expressed by

$$\rho \left[\frac{\partial U}{\partial t} + \mathbf{u}.\nabla U \right] = [\tau : \nabla \mathbf{u} + p\nabla.\mathbf{u}] + \nabla(\kappa \nabla T) \pm \hat{H}_r, \qquad (2.6)$$

where U is the internal energy per unit mass, and H_r is the heat of reaction. By invoking the definition of the internal energy, $dU = C_u dT$, Equation (2.6) becomes,

$$\rho C_v \left(\frac{\partial T}{\partial t} + \mathbf{u}.\nabla T \right) = \tau : \nabla \mathbf{u} + p\nabla.\mathbf{u} + \nabla(\kappa \nabla T) \pm \hat{H}_r. \qquad (2.7)$$

For heat conduction in solids, i.e., when $\mathbf{u} = \mathbf{0}$, $\nabla \mathbf{u} = \mathbf{0}$, and $C_v = C$, the resulting equation is

$$\rho C \frac{\partial T}{\partial t} = \nabla(\kappa \nabla T) \pm \hat{H}_r."$$

Definition 2.4.4. (Newton's Law of Viscosity) [43]

"It states that the shear stress (τ) on a fluid element layer is proportional to the rate of shear strain. The constant of proportionally is called coefficient of viscosity. Mathematically it is expressed as

$$\tau = \mu \frac{du}{dy}.$$

Fluids which obey the above relation are known as Newtonian fluids and the fluids which do not obey the above relation are called Non-Newtonian fluids."

2.5 Dimensionless Parameters

Definition 2.5.1. (Reynolds Number (Re)) [46]

"It is the ratio of the inertial forces to the viscous forces. Based on their behavior, the fluid flows are identified as laminar or turbulent flow. Mathematically, it is expressed as

$$R_e = \frac{\rho U^2}{L} \frac{L^2}{\mu U} \quad \Rightarrow R_e = \frac{LU}{\nu},$$

where U denotes the free stream velocity, L is the characteristics length and ν stands for kinematic viscosity."

Definition 2.5.2. (Nusselt Number (Nu)) [46]

"It is the relationship between the convective to the conductive heat transfer through the boundary of the surface. It is a dimensionless number which was first introduced by the German mathematician Nusselt. Mathematically, it is defined as:

$$N_u = \frac{hL}{\kappa}$$

where h stands for convective heat transfer, L stands for characteristics length and stands for thermal conductivity."

Definition 2.5.3. (Prandtl Number (P_r)) [47]

"The ratio of kinematic diffusivity to heat the diffusivity is said to be Prandtl number. It is denoted by Pr Mathematically, it can be written as

$$P_r = \frac{\nu}{\alpha} \quad \Rightarrow P_r = \frac{\mu c_p}{\rho \kappa},$$

where μ and α denote the momentum diffusivity or kinetic diffusivity and thermal diffusivity respectively. Here c_p denotes the specific heat and κ stands for thermal conductivity."

Definition 2.5.4. (Weissenberg Number (W_e)) [48]

"The Weissenberg number is typically defined as

$$W_e = \frac{\lambda u}{L}$$

where u and L are a characteristic velocity and length scale for the flow. The Weissenberg number indicates the relative importance of fluid elasticity for a given flow problem."

Definition 2.5.5. (Skin Friction Coefficient (C_f)) [48]

"The (skin friction coefficient is typically defined as

$$C_f = \frac{2\tau_w}{\rho w_\infty{}^2},$$

where τ_w is the local wall shear stress, ρ is the fluid density and w_∞ is the free stream velocity (usually taken outside the boundary layer or at the inlet). It expresses the dynamic friction resistance originating in viscous fluid flow around a fixed wall."

Chapter 3

An Unsteady 3D Magnetohydrodynamics Flow of Casson Fluid

3.1 Introduction

The numerical analysis on a 3D incompressible, MHD radiation flow of time-dependent Casson fluid with the radiation and Hall current has been taken into account. Meanwhile The governing coupled nonlinear PDEs are converted into a system of first order ODEs by utilizing the similarity transformations. Furthermore by using shooting technique, the solution of ordinary differential equations are obtained. At the end of this chapter the numerical solution of various parameters have been discussed which impact on the skin friction coefficients, Nusselt number, velocity and temperature. Investigation of obtained numerical results are given through in tables and graphs. The detailed review work of Parshu and Nankeolyar [35] is explain in this chapter.

3.2   Mathematical Modeling

A 3D time-dependent, magnetohydrodynamic flow of an incompressible Casson fluid along a linearly stretchable surface has been examined. Meanwhile, the surface is along the plane, which means that $y = 0$ and the fluid confined along the positive direction of y axis has been considered. Furthermore the sheet is considered to be stretched along x- axis. The time dependent magnetic field has been assumed to act along y-axis which is normal to the surface of sheet. The physical model of flow is given below in Figure 3.1. Here u_w is the stretching sheet velocity along the x-direction, the surface temperature is T_w and the disposition temperature is T_∞. The system of equations describing the flow has been given below, which contains the PDEs of continuity equation, momentum, and energy transfer.
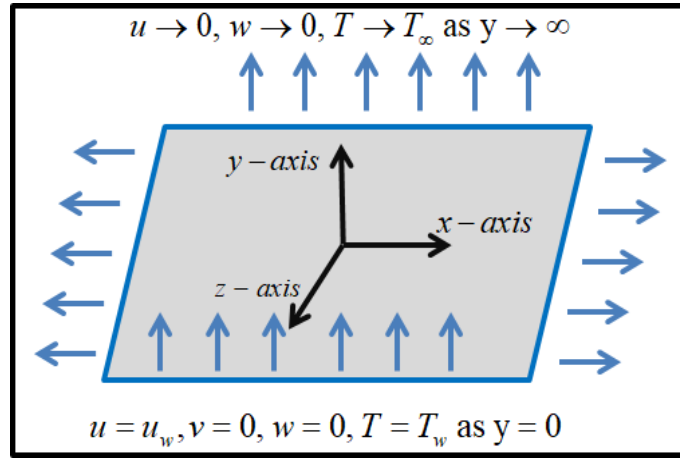

FIGURE 3.1: Schematic representation of physical model.

$$\frac{\partial u}{\partial x} + \frac{\partial v}{\partial y} + \frac{\partial w}{\partial z} = 0, \tag{3.1}$$

$$\frac{\partial u}{\partial t} + u\frac{\partial u}{\partial x} + v\frac{\partial u}{\partial y} + w\frac{\partial u}{\partial z} = \nu\left(1 + \frac{1}{\beta}\right)\frac{\partial^2 u}{\partial y^2} - \frac{\sigma B^2(t)}{\rho(1 + m^2)}(u + mw), \tag{3.2}$$

$$\frac{\partial w}{\partial t} + u\frac{\partial w}{\partial x} + v\frac{\partial w}{\partial y} + w\frac{\partial w}{\partial z} = \nu\left(1 + \frac{1}{\beta}\right)\frac{\partial^2 w}{\partial y^2} + \frac{\sigma B^2(t)}{\rho(1 + m^2)}(mu - w), \tag{3.3}$$

$$\frac{\partial T}{\partial t} + u\frac{\partial T}{\partial x} + v\frac{\partial T}{\partial y} + w\frac{\partial T}{\partial z} = \alpha_m\frac{\partial^2 T}{\partial y^2} - \frac{1}{\rho c_p}\frac{\partial q_r}{\partial y}. \tag{3.4}$$

The associated boundary conditions can be written as:

$$
\left.\begin{array}{l}
y = 0 : u = u_w, v = 0, w = 0, T = T_w, \\[2mm]
y \to \infty : u \to 0, w \to 0, T \to T_\infty.
\end{array}\right\}
\tag{3.5}
$$

The Casson liquid parameter is denoted by β, the electrical conductivity by σ, density by ρ, the kinematic viscosity by ν, Hall current by m, the temperature by T, the thermal diffusivity by $\alpha_m = \frac{k}{\rho c_p}$. Furthermore the wall stretching velocity with time dependent by $u_w(x,t) = \frac{ax}{1-\gamma t}$ and the magnetic field with time dependent by $B(t) = B_0(1-\gamma t)^{-\frac{1}{2}}$, where a and γ are constants and B_0 the magnetic strength. The radiative heat flux q_r can be written as

$$
q_r = -\frac{4\sigma^*}{3\alpha^*}\frac{\partial T^4}{\partial y} = -\frac{16\sigma^*}{3\alpha^*}T^3\frac{\partial T}{\partial y},
\tag{3.6}
$$

where the Stefan-Boltzmann constant is σ^* and the coefficient of Rosseland mean absorption is α^*. From (3.6), putting q_r into (3.4) and after a little simplification, we get

$$
\frac{\partial T}{\partial t} + u\frac{\partial T}{\partial x} + v\frac{\partial T}{\partial y} + w\frac{\partial T}{\partial z} = \frac{\partial}{\partial y}\left(\left(\alpha_m + \frac{16\sigma^* T^3}{3\alpha^* \rho c_p}\right)\frac{\partial T}{\partial y}\right).
\tag{3.7}
$$

For the conversion of the mathematical model(3.1)-(3.4) into the dimensionless form, the following similarity transformation has been introduced,

$$
\left.\begin{array}{l}
u = \dfrac{ax}{1-\gamma t}f'(\eta), \quad v = -\sqrt{\dfrac{a\nu}{1-\gamma t}}f(\eta), \quad w = \dfrac{ax}{1-\gamma t}g(\eta), \\[4mm]
\theta(\eta) = \dfrac{T - T_\infty}{T_f - T_\infty}, \quad \eta = y\sqrt{\dfrac{a}{\nu(1-\gamma t)}}.
\end{array}\right\}
\tag{3.8}
$$

The detailed procedure for the conversion of (3.1)-(3.4) into the dimensionless form has been described in the upcoming discussion.

- $$
\begin{aligned}
\frac{\partial u}{\partial x} &= \frac{\partial}{\partial x}\left(\frac{ax}{1-\gamma t}f'(\eta)\right) \\[2mm]
&= \left(\frac{a}{1-\gamma t}\right)\frac{\partial}{\partial x}(xf')
\end{aligned}
$$

$$= \frac{a}{1-\gamma t}\left[xf''(\eta)\frac{\partial \eta}{\partial x} + f'(\eta)\frac{\partial x}{\partial x}\right]$$

$$= \frac{a}{1-\gamma t}f'(\eta). \tag{3.9}$$

- $$\frac{\partial v}{\partial y} = -\frac{\partial}{\partial y}\left(\sqrt{\frac{a\nu}{1-\gamma t}}f(\eta)\right)$$

$$= -\sqrt{\frac{a\nu}{1-\gamma t}}f'(\eta)\sqrt{\frac{a}{\nu(1-\gamma t)}}$$

$$= -\frac{a}{1-\gamma t}f'(\eta). \tag{3.10}$$

- $$\frac{\partial w}{\partial z} = \frac{\partial}{\partial z}\left(\frac{ax}{1-\gamma t}g(\eta)\right)$$

$$= \frac{ax}{1-\gamma t}\frac{\partial}{\partial z}g(\eta) = 0. \tag{3.11}$$

The (3.1) is very easily satisfied by using the (3.9)-(3.11), as follows

$$\frac{\partial u}{\partial x} + \frac{\partial v}{\partial y} + \frac{\partial w}{\partial z} = \frac{a}{1-\gamma t}f'(\eta) - \frac{a}{1-\gamma t}f'(\eta) + 0 = 0.$$

Now we include the below procedure for the conversion of equation (3.2) into the dimensionless form.

- $$\frac{\partial \eta}{\partial t} = \frac{\partial}{\partial t}\left(y\sqrt{\frac{a}{\nu(1-\gamma t)}}\right)$$

$$= y\sqrt{\frac{a}{\nu}}\left(-\frac{1}{2}(1-\gamma t)^{-\frac{3}{2}}\right)(-\gamma)$$

$$= \frac{\eta}{2}\frac{\gamma}{(1-\gamma t)}.$$

- $$\frac{\partial u}{\partial t} = \frac{\partial}{\partial t}\left(\frac{ax}{1-\gamma t}f'(\eta)\right)$$

$$= ax\left[\frac{1}{1-\gamma t}f''(\eta)\frac{\eta}{2}\frac{\gamma}{(1-\gamma t)} + \frac{\gamma}{(1-\gamma t)^2}f'(\eta)\right]$$

$$= \frac{ax\gamma}{(1-\gamma t)^2}\left(f''(\eta)\frac{\eta}{2}\right) + \frac{ax\gamma}{(1-\gamma t)^2}f'(\eta). \tag{3.12}$$

- $$u\frac{\partial u}{\partial x} = \frac{ax}{1-\gamma t}f'(\eta)\left(\frac{a}{1-\gamma t}f'(\eta)\right)$$

$$= \frac{a^2 x}{(1-\gamma t)^2}(f'(\eta))^2. \tag{3.13}$$

- $$\frac{\partial u}{\partial y} = \frac{\partial}{\partial y}\left(\frac{ax}{1-\gamma t}f'(\eta)\right)$$
  $$= \frac{ax}{1-\gamma t}\sqrt{\frac{a}{\nu(1-\gamma t)}}f''(\eta).$$

- $$v\frac{\partial u}{\partial y} = -\sqrt{\frac{a\nu}{1-\gamma t}}f(\eta)\frac{ax}{1-\gamma t}f''(\eta)\sqrt{\frac{a}{\nu(1-\gamma t)}}$$
  $$= -\frac{a^2 x}{(1-\gamma t)^2}f(\eta)f''(\eta). \qquad (3.14)$$

- $$w\frac{\partial u}{\partial z} = 0. \qquad (3.15)$$

Using (3.12)-(3.15) the left side of (3.2) becomes

$$= \frac{ax\gamma}{(1-\gamma t)^2}\left(f''(\eta)\frac{\eta}{2}\right) + \frac{ax\gamma}{(1-\gamma t)^2}f'(\eta) + \frac{a^2 x}{(1-\gamma t)^2}(f'(\eta)^2) - \frac{a^2 x}{(1-\gamma t)^2}f(\eta)f''(\eta)$$

$$= \frac{ax}{(1-\gamma t)^2}\left(\gamma\frac{\eta}{2}f''(\eta) + \gamma f'(\eta) + a(f'(\eta))^2 - af(\eta)f''(\eta)\right). \qquad (3.16)$$

To convert the right side of equation (3.2) into the dimensionless form, we proceed as follows.

- $$\nu\left(1+\frac{1}{\beta}\right)\frac{\partial^2 u}{\partial y^2} = \nu\left(1+\frac{1}{\beta}\right)\frac{\partial}{\partial y}\left(\frac{ax}{1-\gamma t}f''(\eta)\sqrt{\frac{a}{\nu(1-\gamma t)}}\right)$$
  $$= \left(1+\frac{1}{\beta}\right)\frac{a^2 x}{(1-\gamma t)^2}f'''(\eta). \qquad (3.17)$$

- $$\frac{\sigma B^2(t)}{\rho(1+m^2)}(u+mw) = \frac{\sigma B_0^2}{1-\gamma t}\frac{1}{\rho(1+m^2)}\left(\frac{ax}{1-\gamma t}f'(\eta) + m\frac{ax}{1-\gamma t}g(\eta)\right)$$
  $$= \frac{ax\sigma B_0^2}{(1-\gamma t)^2}\frac{1}{\rho(1+m^2)}\left(f'(\eta)+mg(\eta)\right). \qquad (3.18)$$

Using (3.17)-(3.18), the right side of (3.2) becomes

$$\nu\left(1+\frac{1}{\beta}\right)\frac{\partial^2 u}{\partial y^2} - \frac{\sigma B_0^2(t)}{\rho(1+m^2)}(u+mw)$$

$$= \left(1+\frac{1}{\beta}\right)\frac{a^2 x}{(1-\gamma t)^2}f'''(\eta) - \frac{ax\sigma B_0^2}{(1-\gamma t)^2}\frac{1}{\rho(1+m^2)}\left(f'(\eta)+mg(\eta)\right). \qquad (3.19)$$

Using (3.16) and (3.19), the dimensionless form of (3.2) can be seen as:

$$\frac{ax}{(1-\gamma t)^2}\left(\gamma\frac{\eta}{2}f''(\eta) + \gamma f'(\eta) + a(f'(\eta))^2 - af(\eta)f''(\eta)\right)$$

$$= \left(1+\frac{1}{\beta}\right)\frac{a^2 x}{(1-\gamma t)^2}f'''(\eta) - \frac{ax\sigma B_0^2}{(1-\gamma t)^2}\frac{1}{\rho(1+m^2)}\left(f'(\eta) + mg(\eta)\right).$$

$$\Rightarrow \left(1+\frac{1}{\beta}\right)f''' - \frac{\gamma}{a}\frac{\eta}{2}f'' - \frac{\gamma}{a}f' - (f')^2 + ff'' - \frac{\sigma B_0^2}{a}\frac{1}{\rho(1+m^2)}(f' + mg) = 0.$$

$$(3.20)$$

Now, we include below the procedure for the conversion of equation (3.2) into the dimensionless form

- $$\frac{\partial w}{\partial t} = \frac{\partial}{\partial t}\left(\frac{ax}{1-\gamma t}g(\eta)\right)$$

$$= ax\left(\frac{1}{1-\gamma t}g'(\eta)\frac{\eta}{2}\frac{\gamma}{(1-\gamma t)} + \frac{\gamma}{(1-\gamma t)^2}g(\eta)\right)$$

$$= \frac{ax\gamma}{(1-\gamma t)^2}\frac{\eta}{2}g'(\eta) + \frac{ax\gamma}{(1-\gamma t)^2}g(\eta). \qquad (3.21)$$

- $$u\frac{\partial w}{\partial x} = \frac{ax}{1-\gamma t}f'(\eta)\frac{\partial}{\partial x}\left(\frac{ax}{1-\gamma t}g(\eta)\right)$$

$$= \frac{ax}{1-\gamma t}f'(\eta)\left(\frac{ax}{1-\gamma t}g'(\eta)\frac{\partial\eta}{\partial x} + \frac{a}{1-\gamma t}g(\eta)\right)$$

$$= \frac{a^2 x}{(1-\gamma t)^2}f'(\eta)g(\eta). \qquad \left(\because \frac{\partial\eta}{\partial x} = 0\right) \qquad (3.22)$$

- $$v\frac{\partial w}{\partial y} = -\sqrt{\frac{a\nu}{1-\gamma t}}f(\eta)\frac{\partial}{\partial y}\left(\frac{ax}{1-\gamma t}g(\eta)\right)$$

$$= -\sqrt{\frac{a\nu}{1-\gamma t}}f(\eta)\left(\frac{ax}{1-\gamma t}g'(\eta)\sqrt{\frac{a}{\nu(1-\gamma t)}}\right)$$

$$= -\frac{a^2 x}{(1-\gamma t)^2}f(\eta)g'(\eta). \qquad (3.23)$$

- $$v\frac{\partial w}{\partial z} = \frac{ax}{1-\gamma t}g(\eta)\frac{\partial}{\partial z}\left(\frac{ax}{1-\gamma t}g(\eta)\right) = 0. \qquad (3.24)$$

Using equations (3.21)-(3.24) in left side of (3.3),

$$= \frac{ax\gamma}{(1-\gamma t)^2}\frac{\eta}{2}g'(\eta) + \frac{ax\gamma}{(1-\gamma t)^2}g(\eta) + \frac{a^2 x}{(1-\gamma t)^2}f'(\eta)g(\eta) - \frac{a^2 x}{(1-\gamma t)^2}f(\eta)g'(\eta)$$

$$= \frac{ax}{(1-\gamma t)^2}\left(\gamma\frac{\eta}{2}g'(\eta) + \gamma g(\eta) + af'(\eta)g(\eta) - af(\eta)g'(\eta)\right). \qquad (3.25)$$

To convert the right side of (3.3) into the dimensionless form, the following procedure has been shown.

- $$\nu\left(1+\frac{1}{\beta}\right)\frac{\partial^2 w}{\partial y^2} = \nu\left(1+\frac{1}{\beta}\right)\frac{\partial}{\partial y}\left(\frac{\partial w}{\partial y}\right)$$

$$= \nu\left(1+\frac{1}{\beta}\right)\frac{\partial}{\partial y}\left(\frac{ax}{1-\gamma t}g'(\eta)\sqrt{\frac{a}{\nu(1-\gamma t)}}\right)$$

$$= \nu\left(1+\frac{1}{\beta}\right)\frac{a^2 x}{\nu(1-\gamma t)^2}g''(\eta)$$

$$= \left(1+\frac{1}{\beta}\right)\frac{a^2 x}{(1-\gamma t)^2}g''(\eta). \tag{3.26}$$

- $$\frac{\sigma B^2(t)}{\rho(1+m^2)}(mu-w) = \frac{\sigma B_0^2}{\rho(1+m^2)}\frac{1}{(1-\gamma t)}\left(\frac{max}{(1-\gamma t)}f'(\eta) - \frac{ax}{(1-\gamma t)}g(\eta)\right)$$

$$= \frac{ax}{(1-\gamma t)^2}\frac{\sigma B_0^2}{\rho(1-m^2)}\left(mf'(\eta) - g(\eta)\right). \tag{3.27}$$

Using (3.26)-(3.27) in the right side of (3.3), we get

$$\nu\left(1+\frac{1}{\beta}\right)\frac{\partial^2 w}{\partial y^2} + \frac{\sigma B^2(t)}{\rho(1+m^2)}(mu-w)$$

$$= \left(1+\frac{1}{\beta}\right)\frac{a^2 x}{(1-\gamma t)^2}g''(\eta) + \frac{ax}{(1-\gamma t)^2}\frac{\sigma B_0^2}{\rho(1-m^2)}\left(mf'(\eta) - g(\eta)\right). \tag{3.28}$$

Comparing (3.25) and (3.28), the dimensionless form of equation (3.3) can be written as

$$\frac{ax}{(1-\gamma t)^2}\left(\gamma\frac{\eta}{2}g'(\eta) + \gamma g(\eta) + af'(\eta)g(\eta) - af(\eta)g'(\eta)\right)$$

$$= \left(1+\frac{1}{\beta}\right)\frac{a^2 x}{(1-\gamma t)^2}g''(\eta) + \frac{ax}{(1-\gamma t)^2}\frac{\sigma B_0^2}{\rho(1-m^2)}\left(mf'(\eta) - g(\eta)\right).$$

$$\Rightarrow \left(1+\frac{1}{\beta}\right)g'' - \frac{\gamma}{a}\frac{\eta}{2}g' - \frac{\gamma}{a}g - f'g + fg' + \frac{\sigma B_0^2}{a\rho(1+m^2)}(mf' - g) = 0.$$

$$\tag{3.29}$$

The following derivatives will help to convert the left side of (3.7) into the dimensionless form

- $$\theta(\eta) = \frac{T - T_\infty}{T_w - T_\infty}.$$

$$\Rightarrow \quad T = (T_w - T_\infty)\theta(\eta) + T_\infty.$$

- $$\frac{\partial T}{\partial y} = \frac{\partial}{\partial y}\left((T_w - T_\infty)\theta(\eta)\right)$$

$$= (T_w - T_\infty)\sqrt{\frac{a}{\nu(1 - \gamma t)}}\theta'(\eta)$$

- $$\frac{\partial T}{\partial t} = \frac{\partial}{\partial t}(T_w - T_\infty)\theta(\eta) + T_\infty$$

$$= (T_w - T_\infty)\theta'(\eta)\frac{\partial \eta}{\partial t}$$

$$= (T_w - T_\infty)\frac{\gamma}{(1 - \gamma t)}\frac{\eta}{2}\theta'(\eta). \tag{3.30}$$

- $$u\frac{\partial T}{\partial x} = \frac{ax}{1 - \gamma t}f'(\eta)\frac{\partial}{\partial x}\left((T_w - T_\infty)\theta(\eta)\right) = 0. \tag{3.31}$$

- $$v\frac{\partial T}{\partial y} = -\sqrt{\frac{a\nu}{1 - \gamma t}}f(\eta)(T_w - T_\infty)\sqrt{\frac{a}{\nu(1 - \gamma t)}}\theta'(\eta)$$

$$= -\frac{a}{1 - \gamma t}(T_w - T_\infty)f(\eta)\theta'(\eta). \tag{3.32}$$

- $$w\frac{\partial T}{\partial z} = \frac{ax}{1 - \gamma t}g(\eta)\frac{\partial}{\partial z}\left((T_w - T_\infty)\theta(\eta)\right) = 0. \tag{3.33}$$

Using (3.30)-(3.33) in left side of (3.7) we get

$$= (T_w - T_\infty)\frac{\gamma}{(1 - \gamma t)}\frac{\eta}{2}\theta'(\eta) - \frac{a}{1 - \gamma t}(T_w - T_\infty)f(\eta)\theta'(\eta). \tag{3.34}$$

The dimensionless form of the right side of (3.7) can be obtained as follows

$$\frac{\partial}{\partial y}\left(\left(\alpha_m + \frac{16\sigma^* T^3}{3\alpha^* \rho c_p}\right)\frac{\partial T}{\partial y}\right)$$

$$= \frac{\partial}{\partial y}\left(\left(\alpha_m + \frac{16\sigma^* T^3}{3\alpha^* \rho c_p}\right)(T_w - T_\infty)\sqrt{\frac{a}{\nu(1 - \gamma T)}}\theta'(\eta)\right)$$

$$= (T_w - T_\infty)\sqrt{\frac{a}{\nu(1 - \gamma t)}}\left(\left(\alpha_m + \frac{16\sigma^* T^3}{3\alpha^* \rho c_p}\right)\sqrt{\frac{a}{\nu(1 - \gamma t)}}\theta''(\eta)\right.$$

$$\left. + \theta'(\eta)\frac{16\sigma^*}{3\alpha^* \rho c_p}3T^2(T_w - T_\infty)\sqrt{\frac{a}{\nu(1 - \gamma t)}}\theta'(\eta)\right)$$

$$= (T_w - T_\infty)\frac{a}{\nu(1 - \gamma t)}\left(\left(\alpha_m + \frac{16\sigma^*}{3\alpha^* \rho c_p}T^3\right)\theta''(\eta)\right.$$

$$\left. + \left((T_w - T_\infty)\frac{16\sigma^*}{\alpha^* \rho c_p}T^2\right)(\theta'(\eta))^2\right). \tag{3.35}$$

With the help of (3.34) and (3.35), the dimensionless form of (3.7), is obtained through the following steps:

$$(T_w - T_\infty)\frac{1}{1-\gamma t}\left(\frac{\gamma\eta}{2}\theta'(\eta) - af(\eta)\theta'(\eta)\right)$$

$$= (T_w - T_\infty)\frac{a}{\nu(1-\gamma t)}\left(\left(\alpha_m + \frac{16\sigma^*}{3\alpha^*\rho c_p}T^3\right)\theta''(\eta)\right.$$

$$+ (T_w - T_\infty)\frac{16\sigma^*}{\alpha^*\rho c_p}T^2(\theta'(\eta))^2\right).$$

$$\Rightarrow \frac{\eta}{2}\frac{\gamma}{a}\theta'(\eta) - f(\eta)\theta'(\eta) = \left(\frac{\alpha_m}{\nu} + \frac{16\sigma^*}{3\alpha^*\rho c_p\nu}T^3\right)\theta''(\eta)$$

$$+ (T_w - T_\infty)\frac{16\sigma^*}{\alpha^*\rho c_p\nu}T^2(\theta'(\eta))^2.$$

$$\Rightarrow \left(1 + \frac{4}{3\left(\dfrac{\alpha^*\rho c_p k}{4\sigma^*\rho c_p}\right)}T^3\right)\theta''(\eta) - \frac{\eta}{2}\frac{\gamma\nu}{a\alpha_m}\theta'(\eta) + \frac{\nu}{\alpha_m}f(\eta)\theta'(\eta)$$

$$+ (T_w - T_\infty)\frac{4}{\left(\dfrac{\alpha^*\rho c_p k}{4\sigma^*\rho c_p}\right)}T^2(\theta'(\eta))^2 = 0.$$

$$\Rightarrow \left(1 + \frac{4}{3\left(\dfrac{\alpha^*kT_\infty^3}{4\sigma^*T_\infty^3}\right)}\left(T_\infty + (T_w - T_\infty)\theta(\eta)\right)^3\right)\theta''(\eta) - \frac{\eta}{2}\frac{\gamma}{a}\frac{\nu}{\alpha_m}\theta'(\eta)$$

$$+ \frac{\nu}{\alpha_m}f(\eta)\theta'(\eta) + (T_w - T_\infty)\frac{4}{\left(\dfrac{\alpha^*kT_\infty^3}{4\sigma^*T_\infty^3}\right)}\left(T_\infty + (T_w - T_\infty)\theta(\eta)\right)^2(\theta'(\eta))^2 = 0.$$

$$\Rightarrow \left(1 + \frac{4}{3\left(\dfrac{\alpha^*k}{4\sigma^*T_\infty^3}\right)}\left(1 + \left(\frac{T_w}{T_\infty} - 1\right)\theta\right)^3\right)\theta'' - \frac{\eta}{2}\frac{\gamma}{a}\frac{\nu}{\alpha_m} + \frac{\nu}{\alpha_m}f\theta'$$

$$+ \left(\frac{T_w}{T_\infty} - 1\right)\frac{4}{\left(\dfrac{\alpha^*k}{4\sigma^*T_\infty^3}\right)}\left(1 + \left(\frac{T_w}{T_\infty} - 1\right)\theta\right)^2(\theta')^2 = 0. \tag{3.36}$$

Now for converting the associated boundary conditions into the dimensionless form, the following steps have been taken:

- $u(x, y, z) = u_w$ at $y = 0$.

$$\Rightarrow \frac{ax}{1-\gamma t}f'(\eta) = \frac{ax}{1-\gamma t} \text{ at } \eta = 0.$$

$$\Rightarrow f'(\eta) = 1 \text{ at } \eta = 0.$$

- $v(x, y, z) = 0$ at $y = 0$.

  $\Rightarrow -\sqrt{\dfrac{a\nu}{1 - \gamma t}} f(\eta) = 0$ at $\eta = 0$.

  $\Rightarrow f(\eta) = 0$ at $\eta = 0$.

- $w(x, y, z) = 0$ at $y = 0$.

  $\Rightarrow \dfrac{ax}{1 - \gamma t} g(\eta) = 0$ at $\eta = 0$.

  $\Rightarrow g(\eta) = 0$ at $\eta = 0$.

- $T(x, y, z) = T_w$ at $y = 0$.

  $\Rightarrow (T_w - T_\infty)\theta(\eta) + T_\infty = T_w$ at $\eta = 0$.

  $\Rightarrow (T_w - T_\infty)\theta(\eta) = T_w - T_\infty$ at $\eta = 0$.

  $\Rightarrow \theta(\eta) = 1$ at $\eta = 0$.

- $u(x, y, z) \to 0$ as $y \to \infty$.

  $\Rightarrow \dfrac{ax}{1 - \gamma t} f'(\eta) \to \dfrac{ax}{1 - \gamma t}$ as $\eta \to \infty$.

  $\Rightarrow f'(\eta) \to 0$ as $\eta \to \infty$.

- $w(x, y, z) \to 0$ as $y \to \infty$.

  $\Rightarrow \dfrac{ax}{1 - \gamma t} g(\eta) \to 0$ as $\eta \to \infty$.

  $\Rightarrow g(\eta) \to 0$ as $\eta \to \infty$.

- $T(x, y, z) \to T_\infty$ as $y \to \infty$.

  $\Rightarrow (T_w - T_\infty)\theta(\eta) + T_\infty \to T_\infty$ as $\eta \to \infty$.

  $\Rightarrow (T_w - T_\infty)\theta(\eta) = T_\infty - T_\infty$ as $\eta \to \infty$.

  $\Rightarrow \theta(\eta) \to 0$ as $\eta \to \infty$.

The final dimensionless form of the governing model, is

$$\left(1 + \frac{1}{\beta}\right) f''' + f'' f - (f')^2 - A\left(f' + \frac{\eta}{2} f''\right) - \frac{M}{1 + m^2}(f' + mg) = 0. \qquad (3.37)$$

$$\left(1 + \frac{1}{\beta}\right) g'' - f'g + fg' - A\left(g + \frac{\eta}{2} g'\right) + \frac{M}{1 + m^2}(mf' - g) = 0. \qquad (3.38)$$

$$\left(1 + \frac{4}{3N_r}\left(1 + (tr-1)\theta\right)^3\right)\theta'' - P_r A \frac{\eta}{2}\theta' + P_r f \theta'$$
$$+ \left(\frac{4}{N_r}(tr-1)(1+(tr-1)\theta)^2\right)(\theta')^2 = 0. \tag{3.39}$$

The associated BCs (3.5) shown as

$$\eta = 0: \ f'(\eta) = 1, \ f(\eta) = 0, \ g(\eta) = 0, \ \theta = 1. \tag{3.40}$$

$$\eta \to \infty: \ f'(\eta) \to 0, \ g(\eta) \to 0, \ \theta(\eta) \to 0. \tag{3.41}$$

Different parameters used in (3.37)-(3.39) are defined as follow:

$$A = \frac{\gamma}{a}, \ M = \frac{\sigma B_o^2}{\rho a}, \ N_r = \frac{k\alpha^*}{4\sigma^* T_\infty^3}, \ P_r = \frac{\nu}{\alpha_m}, \ tr = \frac{T_w}{T_\infty}.$$

The skin friction coefficient along x direction, is defined as:

$$C_{fx} = \frac{\tau_{wx}}{\rho u_w^2}. \tag{3.42}$$

To achieve the dimensionless form of C_{fx}, the following steps will be found helpful.

- $\frac{\partial u}{\partial y} = \frac{ax}{1-\gamma t}\sqrt{\frac{a}{\nu(1-\gamma t)}}f''(\eta).$

  $\Rightarrow \left(\frac{\partial u}{\partial y}\right)_{y=0} = \frac{ax}{1-\gamma t}\sqrt{\frac{a}{\nu(1-\gamma t)}}f''(0).$

- $\tau_{wx} = \mu\left(1 + \frac{1}{\beta}\right)\left(\frac{\partial u}{\partial y}\right)_{y=0}$

  $= \mu\left(1 + \frac{1}{\beta}\right)\frac{ax}{1-\gamma t}\sqrt{\frac{a}{\nu(1-\gamma t)}}f''(0). \tag{3.43}$

Using (3.43) in (3.42), we get the following form:

$$C_{fx} = \frac{\mu\left(1+\frac{1}{\beta}\right)\frac{ax}{1-\gamma t}\sqrt{\frac{a}{\nu(1-\gamma t)}}f''(0)}{\rho u_w^2}$$

$$= \frac{\mu\left(1+\frac{1}{\beta}\right)\frac{ax}{1-\gamma t}\sqrt{\frac{a}{\nu(1-\gamma t)}}f''(0)}{\rho\left(\frac{ax}{1-\gamma t}\right)^2} \qquad \left(\because u_w = \frac{ax}{1-\gamma t}\right)$$

$$= \frac{\mu\left(1 + \frac{1}{\beta}\right)\sqrt{\frac{a}{\nu(1 - \gamma t)}}f''(0)}{\rho\left(\frac{ax}{1 - \gamma t}\right)}.$$

$$\Rightarrow \sqrt{Re_x}C_{fx} = \frac{\mu\left(1 + \frac{1}{\beta}\right)\sqrt{\frac{a}{\nu(1 - \gamma t)}}f''(0)}{\rho\left(\frac{ax}{1 - \gamma t}\right)}\sqrt{x\frac{ax}{\nu(1 - \gamma t)}}$$

$$= \mu\left(1 + \frac{1}{\beta}\right)f''(0).$$

The skin friction coefficient along z direction, is defined as:

$$C_{fz} = \frac{\tau_{wz}}{\rho u_w^2}. \tag{3.44}$$

To achieve the dimensionless form of C_{fz}, the following steps will be found helpful.

- $$\frac{\partial w}{\partial y} = \frac{ax}{1 - \gamma t}\sqrt{\frac{a}{\nu(1 - \gamma t)}}g'(\eta)$$

$$\Rightarrow \left(\frac{\partial w}{\partial y}\right)_{y=0} = \frac{ax}{1 - \gamma t}\sqrt{\frac{a}{\nu(1 - \gamma t)}}g'(0)$$

- $$\tau_{wz} = \mu\left(1 + \frac{1}{\beta}\right)\left(\frac{\partial w}{\partial y}\right)_{y=0}$$

$$= \mu\left(1 + \frac{1}{\beta}\right)\frac{ax}{1 - \gamma t}\sqrt{\frac{a}{\nu(1 - \gamma t)}}g'(0). \tag{3.45}$$

Using (3.45) in (3.44), we get the following form:

$$C_{fz} = \frac{\mu\left(1 + \frac{1}{\beta}\right)\frac{ax}{1 - \gamma t}\sqrt{\frac{a}{\nu(1 - \gamma t)}}g'(0)}{\rho u_w^2}$$

$$= \frac{\mu\left(1 + \frac{1}{\beta}\right)\frac{ax}{1 - \gamma t}\sqrt{\frac{a}{\nu(1 - \gamma t)}}g'(0)}{\rho\left(\frac{ax}{1 - \gamma t}\right)^2}$$

$$= \frac{\mu\left(1 + \frac{1}{\beta}\right)\sqrt{\frac{a}{\nu(1 - \gamma t)}}g'(0)}{\rho\left(\frac{ax}{1 - \gamma t}\right)}$$

$$\Rightarrow \sqrt{Re_x}C_{fz} = \frac{\mu\left(1+\dfrac{1}{\beta}\right)\sqrt{\dfrac{a}{\nu(1-\gamma t)}}g'(0)}{\rho\left(\dfrac{ax}{1-\gamma t}\right)}\sqrt{x\dfrac{ax}{\nu(1-\gamma t)}}$$

$$= \mu\left(1+\frac{1}{\beta}\right)g'(0).$$

The local Nusselt number is defined as

$$Nu_x = \frac{xq_w}{k(T_w - T_\infty)}. \tag{3.46}$$

To achieve the dimensionless form of Nu_x, the following steps will be found helpful.

- $q_w(x) = -\left(k\left(\dfrac{\partial T}{\partial y}\right) - q_r\right)_{y=0}$

$$= -\left(k(T_w - T_\infty)\sqrt{\frac{a}{\nu(1-\gamma t)}}\theta'(0)\right.$$
$$\left.+ \frac{16\sigma^*}{3\alpha^*}T^3(T_w - T_\infty)\sqrt{\frac{a}{\nu(1-\gamma t)}}\theta'(0)\right)$$
$$= -(T_w - T_\infty)\sqrt{\frac{a}{\nu(1-\gamma t)}}\theta'(0)\left(K + \frac{16\sigma^*}{3\alpha^*}T^3\right). \tag{3.47}$$

Using (3.47) in (3.46), we get

$$Nu_x = -\frac{x(T_w - T_\infty)\sqrt{\dfrac{a}{\nu(1-\gamma t)}}\theta'(0)\left(K + \dfrac{16\sigma^*}{3\alpha^*}T^3\right)}{k(T_w - T_\infty)}$$

$$= -x\sqrt{\frac{a}{\nu(1-\gamma t)}}\theta'(0)\left(1 + \frac{16\sigma^*}{3\alpha^*k}T^3\right)$$

$$\Rightarrow \frac{Nu_x}{\sqrt{Re_x}} = -\frac{-x\sqrt{\dfrac{a}{\nu(1-\gamma t)}}\theta'(0)\left(1 + \dfrac{16\sigma^*}{3\alpha^*k}T^3\right)}{x\sqrt{\dfrac{a}{(\nu 1-\gamma t)}}}$$

$$= -\left(1 + \frac{4}{3N_r}(1 + (tr-1)\theta(0))^3\right)\theta'(0),$$

where τ_{wx} and τ_{wz} denotes the shear stress components, q_w by the heat transfer rate, and Re_x represents the local Reynolds number defined as $Re_x = \dfrac{xu_w}{\nu}$.

3.3 Method of Solution

For the solution of ODEs (3.37)-(3.39), the shooting method has been used. The dimensionless equations (3.37) and (3.38) are coupled in f and g. These two equations will be solved separately by the shooting method. Later on the solution of (3.37) and (3.38) will be used in (3.39) as a known input. The missing ICs $f''(0)$ and $g'(0)$ are denoted by ξ_1 and ξ_2. For further improvement of the missing conditions, Newton's method will be used. Furthermore, the following notations have been incorporating.

$$\left.\begin{aligned}
&f = y_1, \ f' = y_2, \ f'' = y_3, \ g = y_4, \ g' = y_5, \\
&\frac{\partial f}{\partial \xi_1} = y_6, \ \frac{\partial f'}{\partial \xi_1} = y_7, \ \frac{\partial f''}{\partial \xi_1} = y_8, \ \frac{\partial g}{\partial \xi_1} = y_9, \ \frac{\partial g'}{\partial \xi_1} = y_{10}, \\
&\frac{\partial f}{\partial \xi_2} = y_{11}, \ \frac{\partial f'}{\partial \xi_2} = y_{12}, \ \frac{\partial f''}{\partial \xi_2} = y_{13}, \ \frac{\partial g}{\partial \xi_2} = y_{14}, \ \frac{\partial g'}{\partial \xi_2} = y_{15}.
\end{aligned}\right\}$$

The above mathematical model (3.37)-(3.38), can now be listed in the form of the following first order coupled ODEs.

$$y_1' = y_2, \qquad\qquad\qquad\qquad\qquad\qquad y_1(0) = 0,$$

$$y_2' = y_3, \qquad\qquad\qquad\qquad\qquad\qquad y_2(0) = 1,$$

$$y_3' = \frac{\beta}{\beta+1}\left(A\left(y_2 + \frac{\eta}{2}y_3\right) - y_1 y_3 + y_2^2 + \frac{M}{1+m^2}(y_2 + m y_4)\right), \qquad y_3(0) = \xi_1,$$

$$y_4' = y_5, \qquad\qquad\qquad\qquad\qquad\qquad y_4(0) = 0,$$

$$y_5' = \frac{\beta}{\beta+1}\left(A\left(y_4 + \frac{\eta}{2}y_5\right) + y_4 y_2 - y_1 y_5 - \frac{M}{1+m^2}(m y_2 - y_4)\right), \qquad y_5(0) = \xi_2,$$

$$y_6' = y_7, \qquad\qquad\qquad\qquad\qquad\qquad y_6(0) = 0,$$

$$y_7' = y_8, \qquad\qquad\qquad\qquad\qquad\qquad y_7(0) = 0,$$

$$y_8' = \frac{\beta}{\beta+1}\left(A\left(y_7 + \frac{\eta}{2}y_8\right) - y_1 y_8 - y_3 y_6 + 2 y_2 y_7 + \frac{M}{1+m^2}(y_7 + m y_9)\right),$$

$$y_8(0) = 1,$$

$$y_9' = y_{10}, \qquad\qquad\qquad\qquad\qquad\qquad y_9(0) = 0,$$

$$y'_{10} = \frac{\beta}{\beta+1}\left(A\left(y_9 + \frac{\eta}{2}y_{10}\right) + y_4 y_7 + y_2 y_9 - y_1 y_{10} - y_5 y_6 - \frac{M}{1+m^2}(m y_7 - y_9)\right),$$
$$y_{10}(0) = 0,$$

$$y'_{11} = y_{12}, \qquad\qquad\qquad\qquad\qquad\qquad\qquad\qquad y_{11}(0) = 0,$$

$$y'_{12} = y_{13}, \qquad\qquad\qquad\qquad\qquad\qquad\qquad\qquad y_{12}(0) = 0,$$

$$y'_{13} = \frac{\beta}{\beta+1}\left(A\left(y_{12} + \frac{\eta}{2}y_{13}\right) - y_1 y_{13} - y_3 y_{11} + 2 y_2 y_{12} + \frac{M}{1+m^2}(y_{12} + m y_{14})\right),$$
$$y_{14}(0) = 0,$$

$$y'_{14} = y_{15}, \qquad\qquad\qquad\qquad\qquad\qquad\qquad\qquad y_{14}(0) = 0,$$

$$y'_{15} = \frac{\beta}{\beta+1}\left(A\left(y_{14} + \frac{\eta}{2}y_{15}\right) + y_4 y_{12} + y_2 y_{14} - y_1 y_{15} - y_5 y_{11}\right.$$
$$\left. - \frac{M}{1+m^2}(m y_{12} - y_{14})\right), \qquad\qquad\qquad\qquad\qquad y_{15}(0) = 1.$$

The above IVP will be solved numerically by the RK-4 method. To get the approximate solution, the domain of the problem has been taken as $[0, \eta_\infty]$ instead of $[0, \infty)$, where η_∞ is an appropriate finite positive real number. In the above system of equations, the missing conditions ξ_1 and ξ_2, are to be chosen such that

$$y_2(\eta_\infty, \xi_1, \xi_2) = 0, \quad y_4(\eta_\infty, \xi_1, \xi_2) = 0. \tag{3.48}$$

For the improvement of the missing condition, Newton's method has been implemented which is conducted by the following iterative scheme:

$$\begin{pmatrix} \xi_1^{(k+1)} \\ \xi_2^{(k+1)} \end{pmatrix} = \begin{pmatrix} \xi_1^{(k)} \\ \xi_2^{(k)} \end{pmatrix} - \left[\begin{pmatrix} y_7 & y_9 \\ y_{11} & y_{14} \end{pmatrix}^{-1} \begin{pmatrix} y_2^{(k)} \\ y_4^{(k)} \end{pmatrix} \right]_{\left(\xi_1^{(k)}, \xi_2^{(k)}, \eta_\infty\right)} \tag{3.49}$$

The following steps are involved for the accomplishment of the shooting method.

(i) Choice of the guesses $\xi_1 = \xi_1^{(0)}$ and $\xi_2 = \xi_2^{(0)}$.

(ii) Choice of a positive small number ϵ.

If $max\{|y_2(\eta_\infty - 0)|, |y_4(\eta_\infty - 0)|\} < \epsilon$, stop the process otherwise go to (iii).

(iii) Compute $\xi_1^{(k+1)}$ and $\xi_2^{(k+1)}$, $k = 0, 1, 2, 3....$ by using (3.49).

(iv) Repeat (i) and (ii). In a similar manner, the ODE (3.39) along with the associated BCs can be solved by considering f as a known function.

3.4   Representation of Graphs and Tables

The physical impacts of significant parameters on the skin friction coefficients and Nusselt number have been explained through graphs and tables. Prashu and Nankeolyar [35] used the spectral quasilinearization method (SQLM) for the numerical solution of the discussed model. In the present survey, the shooting method has been opted for reproducing the solution of [35]. The results discussed in Table 3.1, illustrates the impacts of significant parameters on the skin friction coefficients $-C_{fx}Re^{\frac{1}{2}}$ and $C_{fz}Re^{\frac{1}{2}}$. The results are compared with those of Prashu and Nankeolyar [35] showing an excellent agreement. For the rising values of the M the skin friction coefficients increases in both x and z direction. The skin friction coefficient decreases in both x and z direction due to ascending values of the β Casson parameter. Furthermore, the accelerating values of m Hall current decrease the $-C_{fx}Re^{\frac{1}{2}}$ and increase $C_{fz}Re^{\frac{1}{2}}$. Likewise, by increasing the values of unsteadiness A, there is a marginal increment in the skin friction coefficient along the x axis and a decrement along the z axis.

				$-C_{fx}Re^{\frac{1}{2}}$		$C_{fz}Re^{\frac{1}{2}}$	
M	m	A	β	[35]	Present	[35]	Present
6	0.1	0.1	0.3	5.51874456	5.51874456	0.23905696	0.23905696
2				3.63997437	3.63998522	0.12517671	0.12516928
8				6.24973648	6.24973649	0.27988605	0.27988605
	0.5			5.15310039	5.15310038	1.03810463	1.03810463
	1			4.47154368	4.47154408	1.50968576	1.50968577
		0.13		5.52749427	5.52749426	0.23866458	0.23866458
		0.15		5.53332180	5.53332180	0.23840377	0.23840377
			0.5	4.59187303	4.59187303	0.19890741	0.19890741
			0.6	4.32925941	4.32925941	0.18753170	0.18753170

TABLE 3.1:   Results of the $-C_{fx}Re^{\frac{1}{2}}$ and $C_{fz}Re^{\frac{1}{2}}$ for various parameters

In Table 3.2, the effects of the significant parameters on Nusselt number $Nu_xRe^{-\frac{1}{2}}$ have been discussed. The growing pattern is found in the $Nu_xRe^{-\frac{1}{2}}$ due to the accelerating values of m, Prandtl number P_r and temperature ratio tr , while the magnetic parameter M, unsteadiness parameter A and Casson parameter β cause a decrement in the Nusselt number.

							$Nu_x Re^{-\frac{1}{2}}$	
M	m	A	Nr	tr	β	Pr	[35]	Present
6	0.1	0.1	2	1	0.3	10	2.68073953	2.68423226
2							2.85395341	2.85786933
8							2.61197510	2.61530722
	0.5						2.70970177	2.71326368
	1						2.76677553	2.77047595
		0.13					2.64303470	2.64651534
		0.15					2.61732067	2.62079326
			4				2.44614512	2.44976778
			6				2.35862695	2.36229690
				2			3.86324873	3.86589037
				3			5.08255834	5.08427069
					0.5		2.57918784	2.57918784
					0.6		2.54083532	2.54083532
						15	3.39809230	3.40367190
						20	4.00188854	4.00960381

TABLE 3.2: Results of the $Nu_x Re^{-\frac{1}{2}}$ for various parameters.

Figures 3.2-3.4, shows the effects of different parameters on the velocity and temperature respectively. Figure 3.2, shows the decreasing behavior of velocity along the x direction, due to rising values of the β and the M. Actually, the β reveals the properties of yield stress. Stabilization effects are also found by extending the yield stress. The impacts of applied magnetic field give rise to a resistive force in flow field called the Lorentz force. Figure 3.3 reflects that the increasing values of the Casson parameter β and the magnetic field M, the velocity profile along the z-axis increases near the boundary surface and then starts reducing away from the boundary surface. The temperature profile accelerates due to rising values of the β and M which is illustrated in Figure 3.4. Furthermore, the effects of significant parameters, the Hall Current m and the unsteadiness A on the velocity behaviors and the temperature profile are illustrated in Figures 3.5-3.7. When the power of the magnetic field is strong then no one can neglect the effect of Hall current because the utilization of the magnetic field with electrically conducting fluid produces Hall current m. Figures 3.5(a) and (b) illustrate the effects of the m and the A on the velocity profile along the x direction. By ascending values of m, the velocity profile is also increased, while increasing values of the unsteadiness

A, there is a marginal decay in the velocity profile. Figures 3.6 (a) and (b) show the effects of the m and the A on the velocity profile along the z direction. The increasing values of the m, there is a significant rise in the velocity profile, while for the increasing values of the A, there is a marginal decrement in the velocity profile within boundary layer region. Figures 3.7 (a) and (b) show the impact of the m and the A on the temperature. Meanwhile the temperature is a reducing function of the Hall current m and by increasing the values of the unsteadiness A, there is a marginal enhancement in the temperature behavior. By ascending values of the Hall current m, are found to enhance the thickness of the momentum boundary layer. However by accelerating values of the unsteadiness A, the thermal boundary layer becomes thick. The influence of the significant parameters on the temperature behavior is shown in Figures 3.8-3.10 respectively. In Figure 3.8, the rising values of radiative parameter N_r, the temperature is reduced because the temperature distribution is inversely proportion to the N_r, In Figure 3.9 shows that the greater values of Prandtl number P_r has shrink the temperature profile. However P_r is the ratio of the viscous diffusion to the thermal diffusion. Further, Figure 3.10 portrays that the increasing values of temperature ratio tr, the temperature profile shows a growing behavior. Actually tr is a ratio between temperature behavior at the surface to the temperature behavior beyond the surface.

(a)

(b)
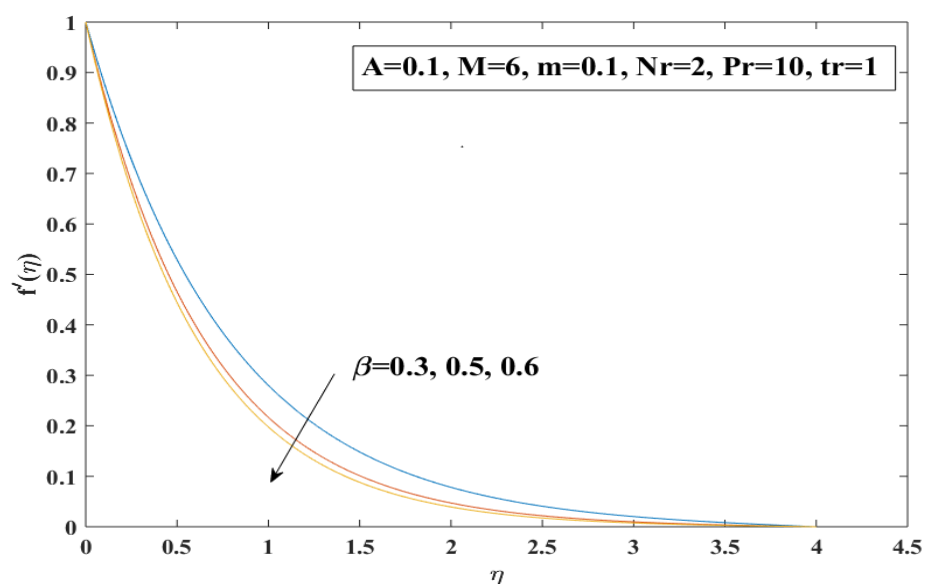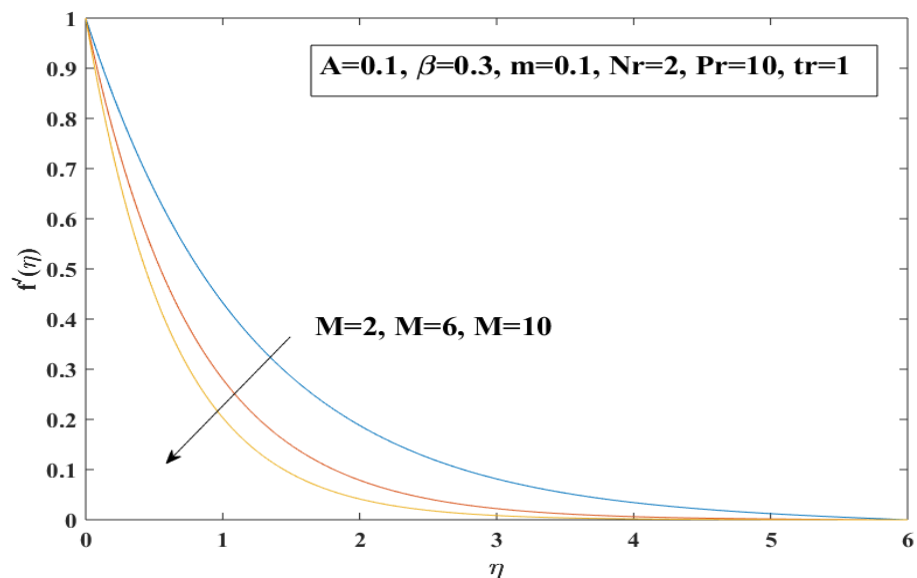
FIGURE 3.2: Change in $f'(\eta)$ for rising values of β and M
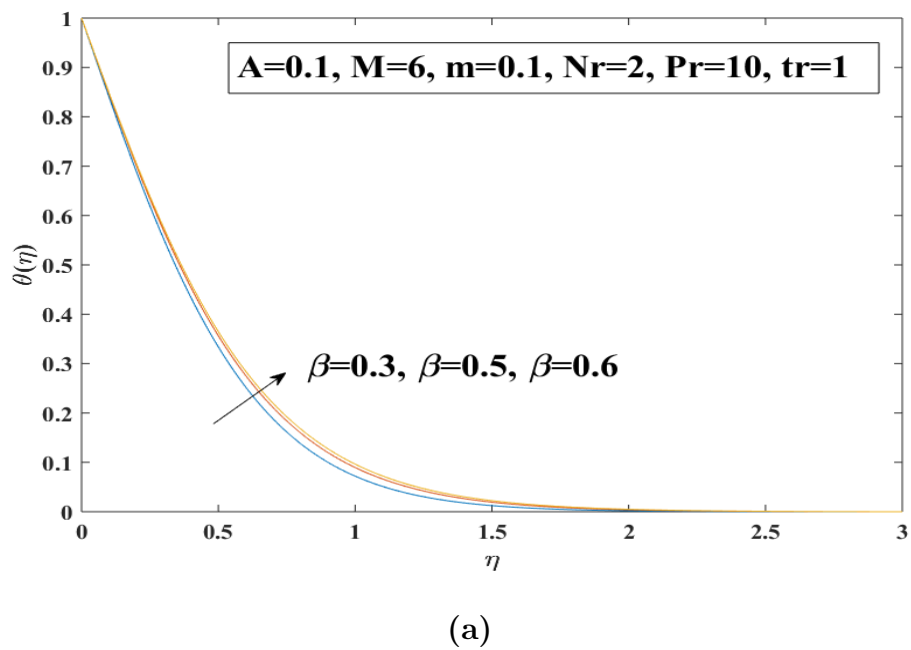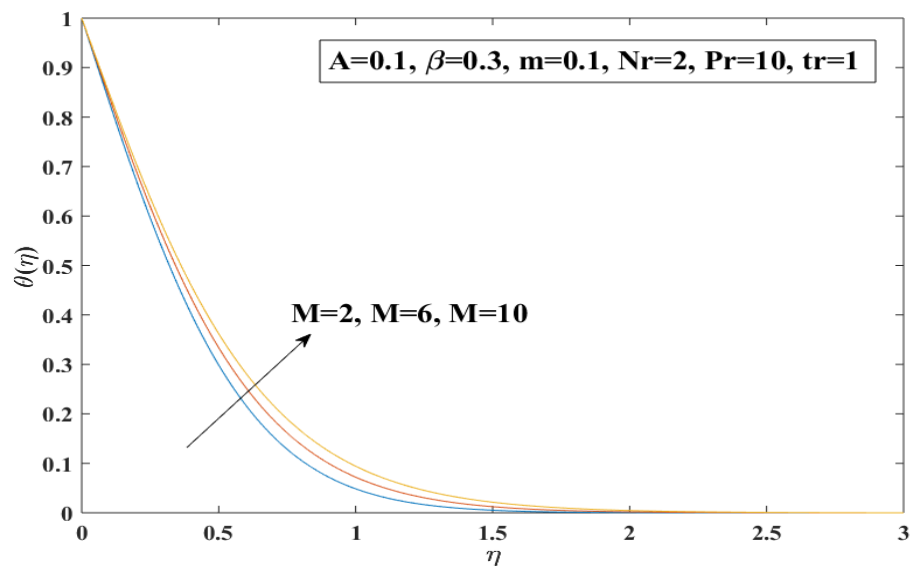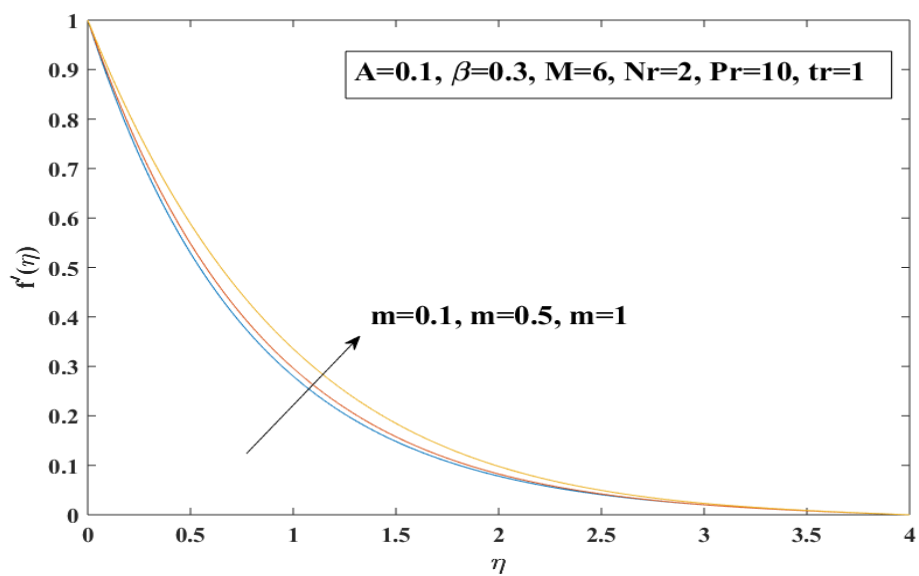

(a)

(b)
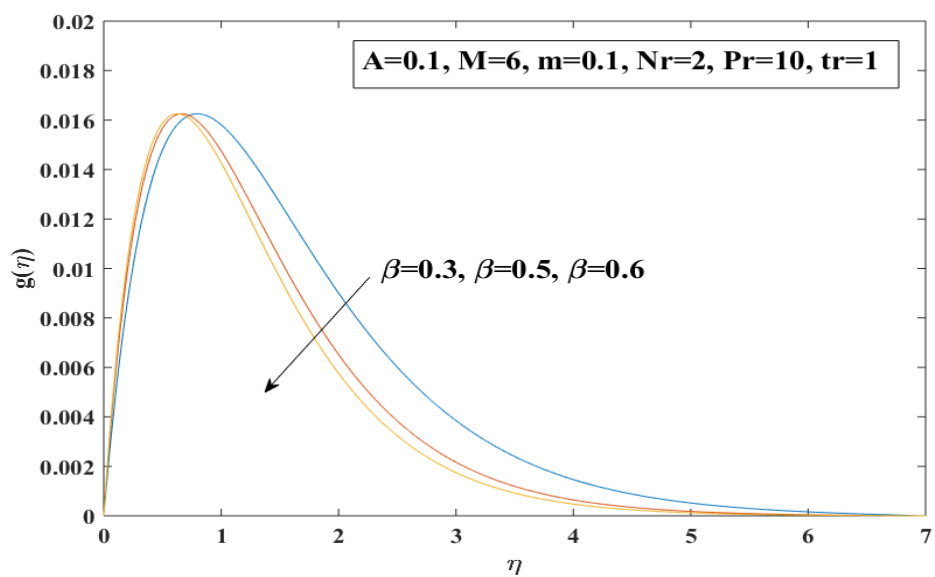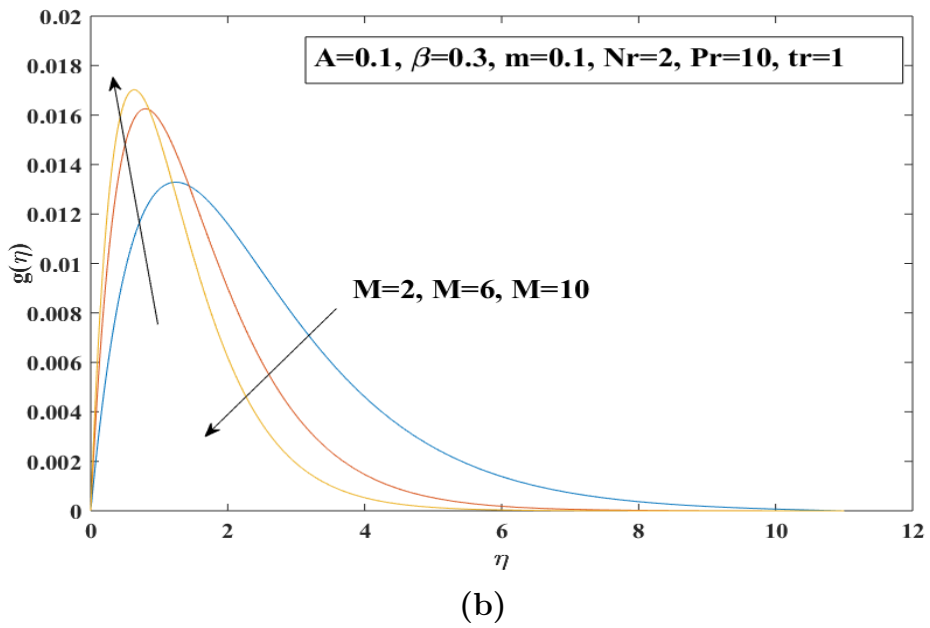
FIGURE 3.3: Change in $g(\eta)$ for rising values of β and M

(a)

(b)

FIGURE 3.4: Change in $\theta(\eta)$ for rising values of β and M
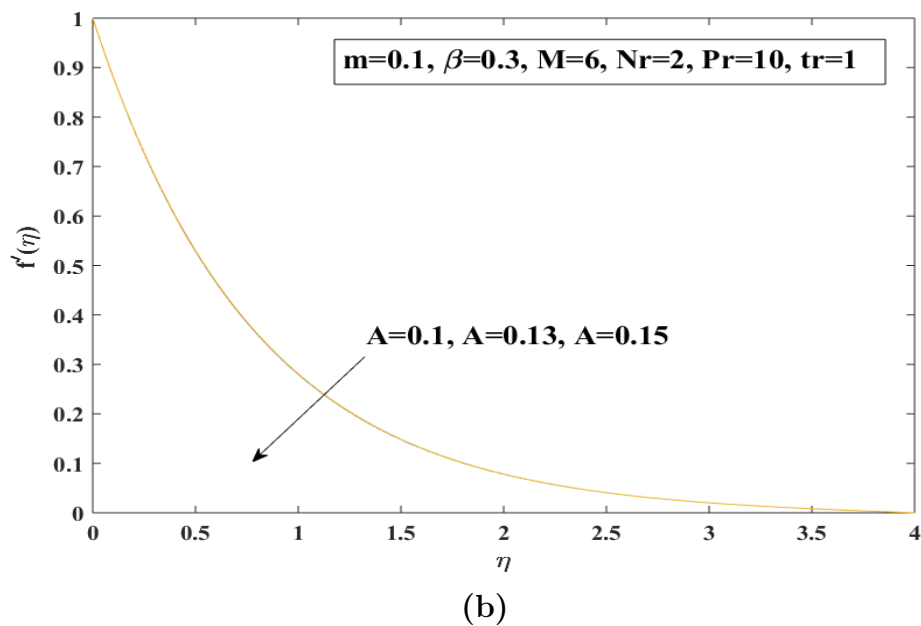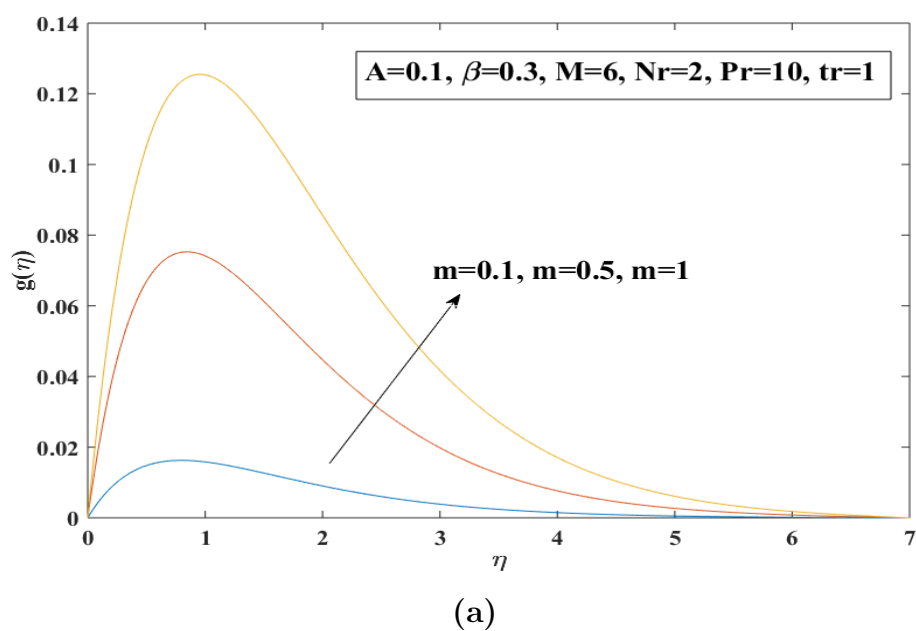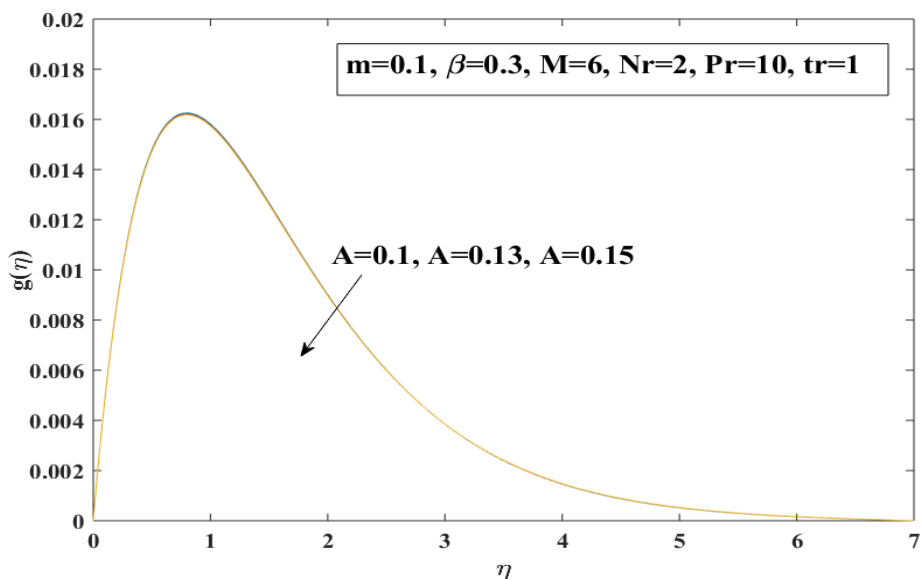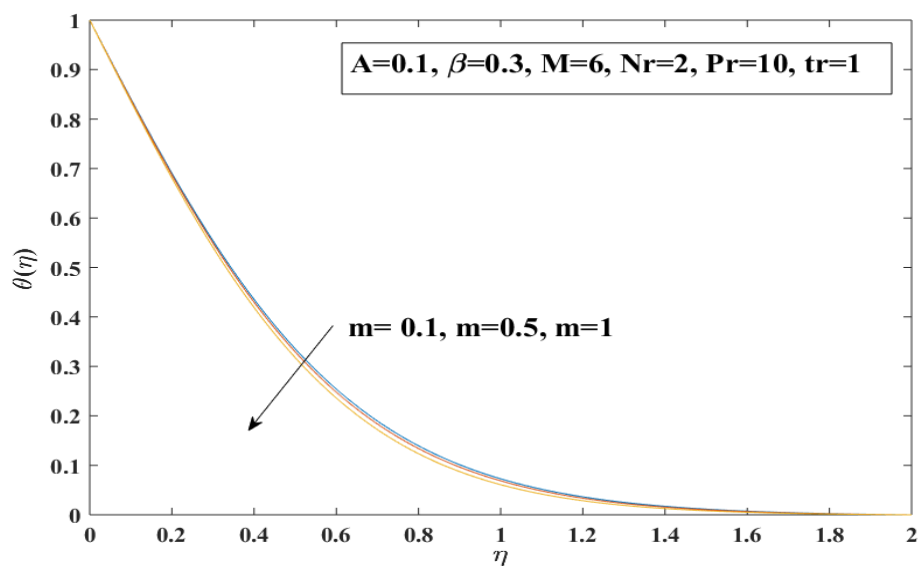

(a)

(b)

FIGURE 3.5: Change in $f'(\eta)$ for rising values of m and A

(a)

(b)

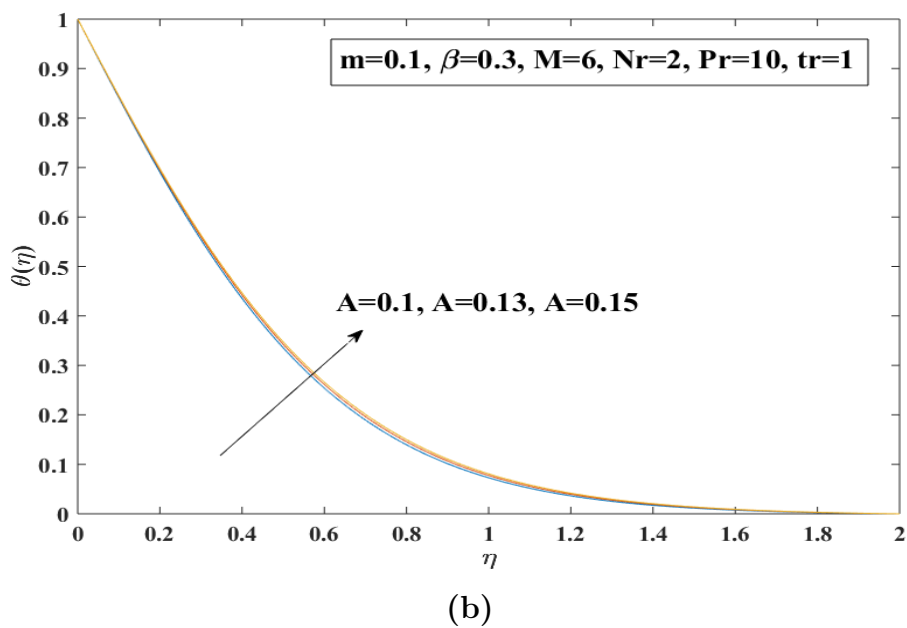FIGURE 3.6: Change in $g(\eta)$ for rising values of m and A

(a)

(b)

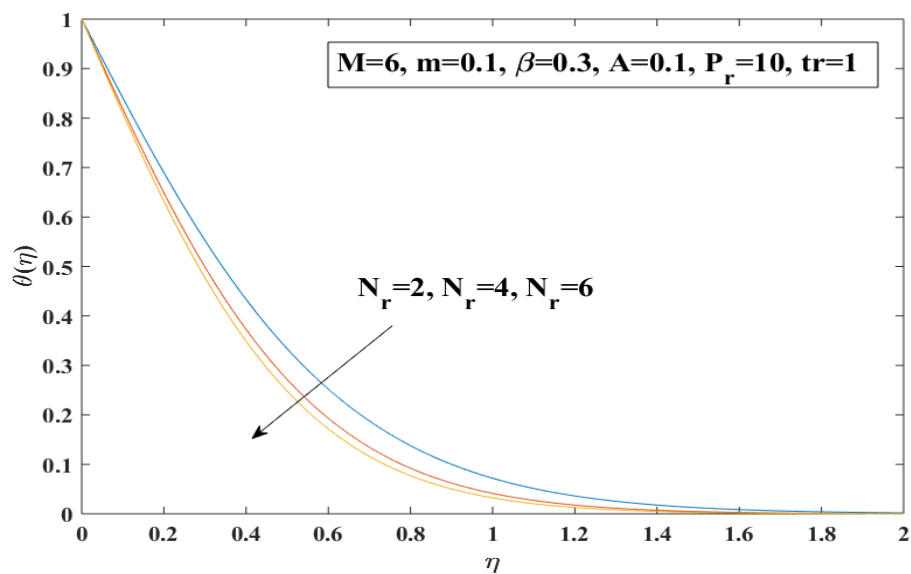FIGURE 3.7: Change in $\theta(\eta)$ for rising values of m and A

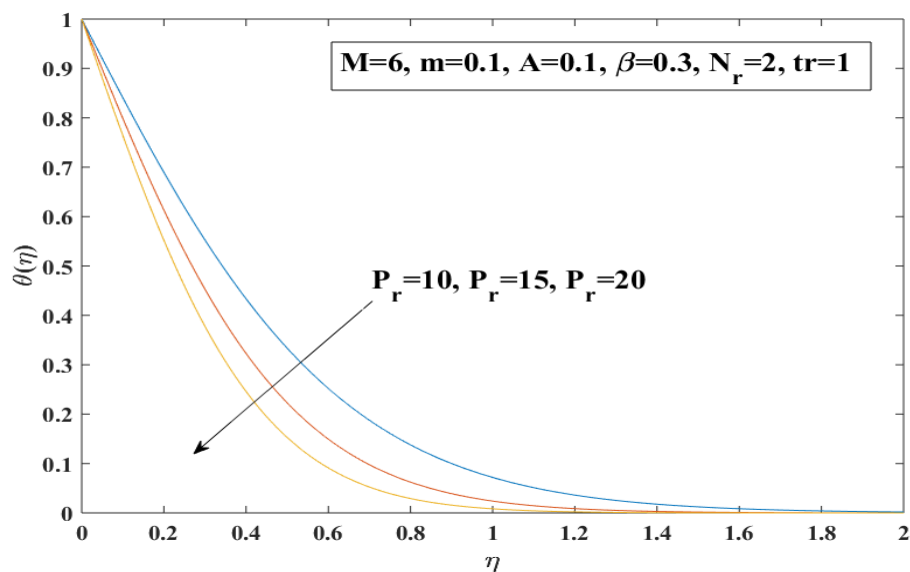FIGURE 3.8: Change in $\theta(\eta)$ for ascending values of N_r

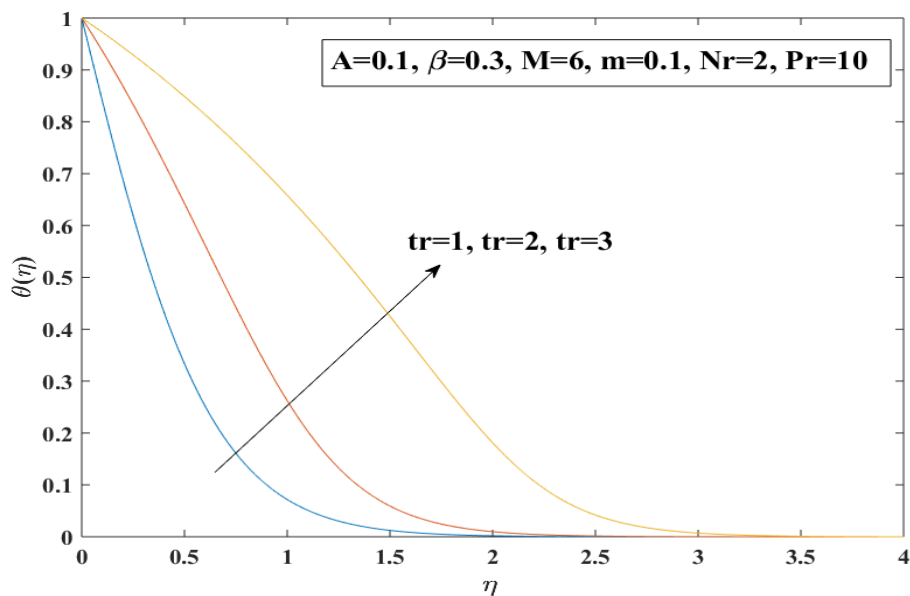FIGURE 3.9: Change in $\theta(\eta)$ for ascending values of P_r

FIGURE 3.10: Change in $\theta(\eta)$ for ascending values of tr

Chapter 4

An Unsteady 3D Magnetohydrodynamics Flow of Carreau Fluid

4.1 Introduction

This chapter contains the extension of [35], by using the Carreau fluid instead of Casson fluid. The numerical investigation on a 3D magnetohydrodynamics flow of an incompressible Carreau fluid along a stretchable sheet has been used. Furthermore, by utilizing the similarity transformations, the nonlinear PDEs are transformed into a set of ODEs. The numerical solution of ordinary differential equations ODEs is obtained by applying numerical technique, the shooting method. The final results are discussed for significant parameters that have impact on the velocity behavior and temperature profile which are presented through in tables and graphs.

4.2   Mathematical Modeling

An unsteady 3D, viscous and incompressible flow of a Carreau fluid along a linearly stretching sheet has been consider. Meanwhile, it is assumed that the $y = 0$ which means that surface is along the plane and the fluid confined the positive direction of y axis. Furthermore the sheet is considered to be stretched along x axis. The time dependent magnetic field has been assumed to act y axis which is normal to the surface of sheet. The physical model of this flow is shown in Figure 4.1. Here u_w is the time dependent wall stretching velocity, the surface temperature is T_w and the disposition temperature is T_∞. The system of equations describing the flow has been given below, which contains the PDEs of continuity equation, momentum, and energy transfer.
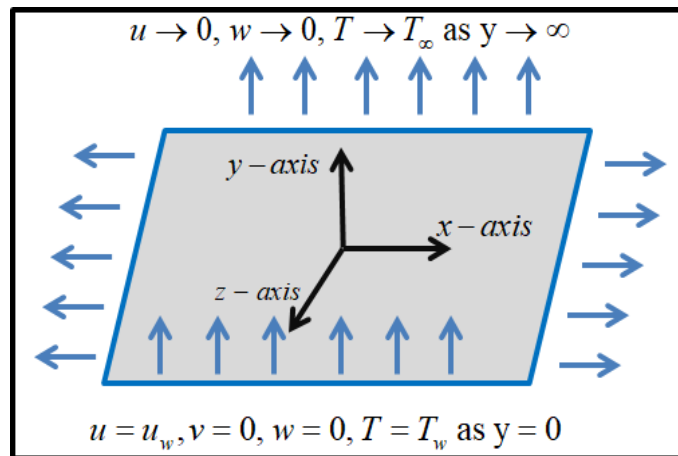

FIGURE 4.1: Schematic representation of physical model.

$$\frac{\partial u}{\partial x} + \frac{\partial v}{\partial y} + \frac{\partial w}{\partial z} = 0, \tag{4.1}$$

$$\frac{\partial u}{\partial t} + u\frac{\partial u}{\partial x} + v\frac{\partial u}{\partial y} + w\frac{\partial u}{\partial z} = \nu\left(1 + \frac{3(n-1)}{2}\Gamma^2\left(\frac{\partial u}{\partial y}\right)^2\right)\frac{\partial^2 u}{\partial y^2}$$
$$- \frac{\sigma B^2(t)}{\rho(1+m^2)}(u + mw), \tag{4.2}$$

$$\frac{\partial w}{\partial t} + u\frac{\partial w}{\partial x} + v\frac{\partial w}{\partial y} + w\frac{\partial w}{\partial z} = \nu\left(1 + \frac{3(n-1)}{2}\Gamma^2\left(\frac{\partial w}{\partial y}\right)^2\right)\frac{\partial^2 w}{\partial y^2}$$
$$+ \frac{\sigma B^2(t)}{\rho(1+m^2)}(mu - w), \tag{4.3}$$

$$\frac{\partial T}{\partial t} + u\frac{\partial T}{\partial x} + v\frac{\partial T}{\partial y} + w\frac{\partial T}{\partial z} = \alpha_m\frac{\partial^2 T}{\partial y^2} - \frac{1}{\rho c_p}\frac{\partial q_r}{\partial y}. \tag{4.4}$$

The associated BCs can be written as:

$$
\left.\begin{aligned}
y = 0 : u = u_w, v = 0, w = 0, T = T_w, \\
y \to \infty : u \to 0, w \to 0, T \to T_\infty.
\end{aligned}\right\}
\tag{4.5}
$$

In the above model, the power-law index is denoted by n, the time constant by Γ, the electrical conductivity by σ, density by ρ, the kinematic viscosity by ν, Hall current by m, the temperature by T, the thermal diffusivity by $\alpha_m = \frac{k}{\rho c_p}$ and the stretching sheet velocity in x-direction by u_w. Furthermore the wall stretching velocity has been taken as $u_w(x,t) = \frac{ax}{1-\gamma t}$ and the magnetic field with time dependent as $B(t) = B_0(1 - \gamma t)^{-\frac{1}{2}}$, where a and γ are constants and B_0 the magnetic strength.

For the conversion of the mathematical model (4.1) and (4.4) into the dimensionless form, the following similarity transformation has been introduced.

$$
\left.\begin{aligned}
u = \frac{ax}{1 - \gamma t} f'(\eta), \quad v = -\sqrt{\frac{a\nu}{1 - \gamma t}} f(\eta), \quad w = \frac{ax}{1 - \gamma t} g(\eta), \\
\theta(\eta) = \frac{T - T_\infty}{T_f - T_\infty}, \quad \eta = y\sqrt{\frac{a}{\nu(1 - \gamma t)}}.
\end{aligned}\right\}
\tag{4.6}
$$

The detailed procedure for the conversion of continuity equation (4.1) has been discussed in Chapter 3.

Now, we include the below procedure for the conversion of equation (4.2) into the dimensionless form. The left side of equation (4.2) can be written as:

$$
= \frac{ax}{(1 - \gamma t)^2} \left(\gamma \frac{\eta}{2} f''(\eta) + \gamma f'(\eta) + a(f'(\eta))^2 - af(\eta)f''(\eta) \right).
\tag{4.7}
$$

To convert the right side of equation (4.2) into the dimensionless form, we proceed as follows.

- $\nu \left(1 + \frac{3(n-1)}{2} \Gamma^2 \left(\frac{\partial u}{\partial y} \right)^2 \right) \frac{\partial^2 u}{\partial y^2}$

$$
= \nu \left(1 + \frac{3(n-1)}{2} \Gamma^2 \left(\frac{ax}{1 - \gamma t} f''(\eta) \sqrt{\frac{a}{\nu(1 - \gamma t)}} \right)^2 \right) \frac{\partial}{\partial y} \left(\frac{ax}{1 - \gamma t} f''(\eta) \sqrt{\frac{a}{(1 - \gamma t)}} \right)
$$

$$
= \left(1 + \frac{3(n-1)}{2} \Gamma^2 \frac{a^3 x^2}{\nu(1 - \gamma t)^3} (f''(\eta))^2 \right) \frac{a^2 x}{(1 - \gamma t)^2} f'''(\eta).
\tag{4.8}
$$

$$\bullet \quad \frac{\sigma B^2(t)}{\rho(1+m^2)}(u+mw)$$

$$= \frac{\sigma B_0^2}{1-\gamma t}\frac{1}{\rho(1+m^2)}\left(\frac{ax}{1-\gamma t}f'(\eta) + m\frac{ax}{1-\gamma t}g(\eta)\right)$$

$$= \frac{ax\sigma B_0^2}{(1-\gamma t)^2}\frac{1}{\rho(1+m^2)}\left(f'(\eta) + mg(\eta)\right). \tag{4.9}$$

Using (4.8)-(4.9), the right side of equation (4.2) becomes:

$$\nu\left(1 + \frac{3(n-1)}{2}\Gamma^2\left(\frac{\partial u}{\partial y}\right)^2\right)\frac{\partial^2 u}{\partial y^2} - \frac{\sigma B_0^2(t)}{\rho(1+m^2)}(u+mw)$$

$$= \left(1 + \frac{3(n-1)}{2}\Gamma^2\frac{a^3 x^2}{\nu(1-\gamma t)^3}f''(\eta)^2\right)\frac{a^2 x}{(1-\gamma t)^2}f'''(\eta)$$

$$- \frac{ax\sigma B_0^2}{(1-\gamma t)^2}\frac{1}{\rho(1+m^2)}\left(f'(\eta) + mg(\eta)\right). \tag{4.10}$$

Using (4.7) and (4.10) the dimensionless form of equation (4.2) can be seen as:

$$\frac{ax}{(1-\gamma t)^2}\left(\gamma\frac{\eta}{2}f''(\eta) + \gamma f'(\eta) + a(f'(\eta))^2 - af(\eta)f''(\eta)\right)$$

$$= \left(1 + \frac{3(n-1)}{2}\Gamma^2\frac{a^3 x^2}{\nu(1-\gamma t)^3}f''(\eta)^2\right)\frac{a^2 x}{(1-\gamma t)^2}f'''(\eta)$$

$$- \frac{ax\sigma B_0^2}{(1-\gamma t)^2}\frac{1}{\rho(1+m^2)}\left(f'(\eta) + mg(\eta)\right).$$

$$\Rightarrow \left(1 + \frac{3(n-1)}{2}\Gamma^2\frac{a^3 x^2}{\nu(1-\gamma t)^3}(f'')^2\right)f''' - \frac{\gamma}{a}\frac{\eta}{2}f'' - \frac{\gamma}{a}f' - (f')^2 + ff''$$

$$- \frac{\sigma B_0^2}{a}\frac{1}{\rho(1+m^2)}(f' + mg) = 0. \tag{4.11}$$

Now, we include below the procedure for the conversion of equation (4.3) into the dimensionless form. The left side of equation (4.3) can be written as:

$$= \frac{ax}{(1-\gamma t)^2}\left(\gamma\frac{\eta}{2}g'(\eta) + \gamma g(\eta) + af'(\eta)g(\eta) - af(\eta)g'(\eta)\right) \tag{4.12}$$

To convert the right side of (4.3) into the dimensionless form, the following procedure has been shown.

$$\bullet \quad \nu\left(1 + \frac{3(n-1)}{2}\Gamma^2\left(\frac{\partial w}{\partial y}\right)^2\right)\frac{\partial^2 w}{\partial y^2}$$

$$= \nu \left(1 + \frac{3(n-1)}{2} \Gamma^2 \left(\frac{ax}{1-\gamma t} g'(\eta) \sqrt{\frac{a}{\nu(1-\gamma t)}} \right)^2 \right) \frac{a^2 x}{\nu(1-\gamma t)^2} g''(\eta).$$

$$= \left(1 + \frac{3(n-1)}{2} \Gamma^2 \left(\frac{a^3 x^2}{(1-\gamma t)^3} (g'(\eta))^2 \right) \right) \frac{a^2 x}{(1-\gamma t)^2} g''(\eta). \tag{4.13}$$

- $\dfrac{\sigma B^2(t)}{\rho(1+m^2)}(mu - w)$

$$= \frac{\sigma B_0^2}{\rho(1+m^2)} \frac{1}{(1-\gamma t)} \left(\frac{max}{(1-\gamma t)} f'(\eta) - \frac{ax}{(1-\gamma t)} g(\eta) \right)$$

$$= \frac{ax}{(1-\gamma t)^2} \frac{\sigma B_0^2}{\rho(1-m^2)} \left(m f'(\eta) - g(\eta) \right). \tag{4.14}$$

Using (4.13)-(4.14) in the right side of (4.3), we get

$$\nu \left(1 + \frac{3(n-1)}{2} \Gamma^2 \left(\frac{\partial w}{\partial y} \right)^2 \right) \frac{\partial^2 w}{\partial y^2} + \frac{\sigma B^2(t)}{\rho(1+m^2)}(mu - w)$$

$$= \left(1 + \frac{3(n-1)}{2} \Gamma^2 \left(\frac{a^3 x^2}{(1-\gamma t)^3} (g'(\eta))^2 \right) \right) \frac{a^2 x}{(1-\gamma t)^2} g''(\eta)$$

$$+ \frac{ax}{(1-\gamma t)^2} \frac{\sigma B_0^2}{\rho(1-m^2)} \left(m f'(\eta) - g(\eta) \right). \tag{4.15}$$

Comparing (4.12) and (4.15), the dimensionless form of equation (4.3) can be written as:

$$\frac{ax}{(1-\gamma t)^2} \left(\gamma \frac{\eta}{2} g'(\eta) + \gamma g(\eta) + a f'(\eta) g(\eta) - a f(\eta) g'(\eta) \right)$$

$$= \left(1 + \frac{3(n-1)}{2} \Gamma^2 \left(\frac{a^3 x^2}{(1-\gamma t)^3} (g'(\eta))^2 \right) \right) \frac{a^2 x}{(1-\gamma t)^2} g''(\eta)$$

$$+ \frac{ax}{(1-\gamma t)^2} \frac{\sigma B_0^2}{\rho(1-m^2)} \left(m f'(\eta) - g(\eta) \right).$$

$$\Rightarrow \left(1 + \frac{3(n-1)}{2} \Gamma^2 \left(\frac{a^3 x^2}{(1-\gamma t)^3} (g')^2 \right) \right) g'' - \frac{\gamma}{a} \frac{\eta}{2} g' - \frac{\gamma}{a} g - f' g + f g'$$

$$+ \frac{\sigma B_0^2}{a\rho(1+m^2)} (m f' - g) = 0. \tag{4.16}$$

The detailed procedure for the conversion of equation (4.4) into dimensionless form is similar to that discussed in chapter 3. The final dimensionless form of the governing model, is

$$\left(1 + \frac{3(n-1)}{2}We(f'')^2\right)f''' + f''f - (f')^2 - A\left(f' + \frac{\eta}{2}f''\right)$$

$$- \frac{M}{1+m^2}(f' + mg) = 0. \tag{4.17}$$

$$\left(1 + \frac{3(n-1)}{2}We(g')^2\right)g'' - f'g + fg' - A\left(g + \frac{\eta}{2}g'\right)$$

$$+ \frac{M}{1+m^2}(mf' - g) = 0. \tag{4.18}$$

$$\left(1 + \frac{4}{3N_r}\left(1 + (tr-1)\theta\right)^3\right)\theta'' - P_rA\frac{\eta}{2}\theta' + P_rf\theta'$$

$$+ \left(\frac{4}{N_r}(tr-1)(1 + (tr-1)\theta)^2\right)(\theta')^2 = 0. \tag{4.19}$$

The converted form of the associated BCs (4.5) is:

$$\eta = 0 : \ f' = 1, \ f = 0, \ g = 0, \ \theta = 1. \tag{4.20}$$

$$\eta \to \infty : \ f' \to 0, \ g \to 0, \ \theta \to 0. \tag{4.21}$$

The skin friction coefficient in x-direction, is defined as:

$$C_{fx} = \frac{\tau_{wx}}{\rho u_w^2}. \tag{4.22}$$

To achieve the dimensionless form of C_{fx}, the following steps will be found helpful.

- $$\frac{\partial u}{\partial y} = \frac{ax}{1 - \gamma t}\sqrt{\frac{a}{\nu(1 - \gamma t)}}f''(\eta).$$

$$\Rightarrow \left(\frac{\partial u}{\partial y}\right)_{y=0} = \frac{ax}{1 - \gamma t}\sqrt{\frac{a}{\nu(1 - \gamma t)}}f''(0).$$

$$\Rightarrow \left(\frac{\partial u}{\partial y}\right)_{y=0}^2 = \frac{a^3x^2}{(1 - \gamma t)^3}(f''(0))^2.$$

- $$\tau_{wx} = \mu\left(1 + \Gamma^2\frac{(n-1)}{2}\left(\frac{\partial u}{\partial y}\right)^2\right)\left(\frac{\partial u}{\partial y}\right)_{y=0}$$

$$= \mu\left(1 + \frac{n-1}{2}\frac{\Gamma^2a^3x^2}{\nu(1 - \gamma t)^3}(f''(0))^2\right)\frac{ax}{1 - \gamma t}\sqrt{\frac{a}{\nu(1 - \gamma t)}}f''(0) \tag{4.23}$$

Using (4.23) in (4.22), we get the following form:

$$C_{fx} = \frac{\mu\left(1 + \dfrac{n-1}{2}\dfrac{\Gamma^2 a^3 x^2}{\nu(1-\gamma t)^3}(f''(0))^2\right)\dfrac{ax}{1-\gamma t}\sqrt{\dfrac{a}{\nu(1-\gamma t)}}f''(0)}{\rho u_w^2}$$

$$= \frac{\mu\left(1 + \dfrac{n-1}{2}\dfrac{\Gamma^2 a^3 x^2}{\nu(1-\gamma t)^3}(f''(0))^2\right)\dfrac{ax}{1-\gamma t}\sqrt{\dfrac{a}{\nu(1-\gamma t)}}f''(0)}{\rho\left(\dfrac{ax}{1-\gamma t}\right)^2}$$

$$= \frac{\mu\left(1 + \dfrac{n-1}{2}\dfrac{\Gamma^2 a^3 x^2}{\nu(1-\gamma t)^3}(f''(0))^2\right)\sqrt{\dfrac{a}{\nu(1-\gamma t)}}f''(0)}{\rho\left(\dfrac{ax}{1-\gamma t}\right)}.$$

$$\Rightarrow \sqrt{Re_x}\,C_{fx} = \frac{\mu\left(1 + \dfrac{n-1}{2}We(f''(0))^2\right)\sqrt{\dfrac{a}{\nu(1-\gamma t)}}f''(0)}{\rho\left(\dfrac{ax}{1-\gamma t}\right)}\sqrt{x\dfrac{ax}{\nu(1-\gamma t)}}$$

$$= \left(1 + \dfrac{n-1}{2}We(f''(0))^2\right)f''(0).$$

The skin friction coefficient in z-direction, is defined as:

$$C_{fz} = \frac{\tau_{wz}}{\rho u_w^2}. \tag{4.24}$$

To achieve the dimensionless form of C_{fz}, the following steps are found useful.

- $\dfrac{\partial w}{\partial y} = \dfrac{ax}{1-\gamma t}\sqrt{\dfrac{a}{\nu(1-\gamma t)}}g'(\eta)$

  $\Rightarrow \left(\dfrac{\partial w}{\partial y}\right)_{y=0} = \dfrac{ax}{1-\gamma t}\sqrt{\dfrac{a}{\nu(1-\gamma t)}}g'(0)$

  $\Rightarrow \left(\dfrac{\partial w}{\partial y}\right)^2_{y=0} = \dfrac{a^3 x^2}{\nu(1-\gamma t)^3}(g'(0))^2.$

- $\tau_{wx} = \mu\left(1 + \Gamma^2\dfrac{(n-1)}{2}\left(\dfrac{\partial w}{\partial y}\right)^2\right)\left(\dfrac{\partial w}{\partial y}\right)_{y=0}$

  $= \mu\left(1 + \dfrac{n-1}{2}\dfrac{\Gamma^2 a^3 x^2}{\nu(1-\gamma t)^3}(g'(0))^2\right)\dfrac{ax}{1-\gamma t}\sqrt{\dfrac{a}{\nu(1-\gamma t)}}g'(0).$ (4.25)

Using (4.25) in (4.24), we get the following form:

$$C_{fz} = \frac{\mu\left(1 + \dfrac{n-1}{2}\dfrac{\Gamma^2 a^3 x^2}{\nu(1-\gamma t)^3}(g'(0))^2\right)\dfrac{ax}{1-\gamma t}\sqrt{\dfrac{a}{\nu(1-\gamma t)}}g'(0)}{\rho u_w^2}$$

$$= \frac{\mu\left(1 + \dfrac{n-1}{2}\dfrac{\Gamma^2 a^3 x^2}{\nu(1-\gamma t)^3}(g'(0))^2\right)\dfrac{ax}{1-\gamma t}\sqrt{\dfrac{a}{\nu(1-\gamma t)}}g'(0)}{\rho\left(\dfrac{ax}{1-\gamma t}\right)^2}$$

$$= \frac{\mu\left(1 + \dfrac{n-1}{2}\dfrac{\Gamma^2 a^3 x^2}{\nu(1-\gamma t)^3}(g'(0))^2\right)\dfrac{ax}{1-\gamma t}\sqrt{\dfrac{a}{\nu(1-\gamma t)}}g'(0)}{\rho\left(\dfrac{ax}{1-\gamma t}\right)}.$$

$$\Rightarrow \sqrt{Re_x}\,C_{fz} = \frac{\mu\left(1 + \dfrac{n-1}{2}We(f'(0))^2\right)\sqrt{\dfrac{a}{\nu(1-\gamma t)}}g'(0)}{\rho\left(\dfrac{ax}{1-\gamma t}\right)}\sqrt{x\dfrac{ax}{\nu(1-\gamma t)}}$$

$$= \left(1 + \dfrac{n-1}{2}We(g'(0))^2\right)g'(0).$$

The detailed procedure for the conversion of local Nusselt number in dimensionless form is similar to that discussed in chapter 3.

4.3   Method of Solution

In order to solve the system of ODEs (4.17) and (4.18), the shooting method has been used. The dimensionless equations (4.17) and (4.18) are coupled in f and g. These two equations will be solved separately by the shooting method. Later on, the solution of (4.17) and (4.18) will be used in (4.19) as a known input. The missing initial conditions $f''(0)$ and $g'(0)$ are denoted by ξ_1 and ξ_2. For further improvement of the missing conditions, Newton's method will be used.

Furthermore, the following notations have been incorporating.

$$
\left.
\begin{aligned}
&f = y_1, \ f' = y_2, \ f'' = y_3, \ g = y_4, \ g' = y_5, \\
&\frac{\partial f}{\partial \xi_1} = y_6, \ \frac{\partial f'}{\partial \xi_1} = y_7, \ \frac{\partial f''}{\partial \xi_1} = y_8, \ \frac{\partial g}{\partial \xi_1} = y_9, \ \frac{\partial g'}{\partial \xi_1} = y_{10}, \\
&\frac{\partial f}{\partial \xi_2} = y_{11}, \ \frac{\partial f'}{\partial \xi_2} = y_{12}, \ \frac{\partial f''}{\partial \xi_2} = y_{13}, \ \frac{\partial g}{\partial \xi_2} = y_{14}, \ \frac{\partial g'}{\partial \xi_2} = y_{15}.
\end{aligned}
\right\}
$$

For simplification, the following notation have been defined.

$$
1 + \frac{3(n-1)}{2} We(y_3)^2 = \phi_1
$$
$$
1 + \frac{3(n-1)}{2} We(y_5)^2 = \phi_2 \tag{4.26}
$$

The system of equations (4.17)-(4.18), can now be written in the form of the following first order coupled ODEs.

$$
\begin{aligned}
y_1' =& y_2, & y_1(0) &= 0, \\[2mm]
y_2' =& y_3, & y_2(0) &= 1, \\[2mm]
y_3' =& \frac{1}{\phi_1}\left(A\left(y_2 + \frac{\eta}{2}y_3\right) - y_1 y_3 + y_2^2 + \frac{M}{1+m^2}(y_2 + my_4) \right), & y_3(0) &= \xi_1, \\[2mm]
y_4' =& y_5, & y_4(0) &= 0, \\[2mm]
y_5' =& \frac{1}{\phi_2}\left(A\left(y_4 + \frac{\eta}{2}y_5\right) + y_4 y_2 - y_1 y_5 - \frac{M}{1+m^2}(my_2 - y_4) \right), & y_5(0) &= \xi_2, \\[2mm]
y_6' =& y_7, & y_6(0) &= 0, \\[2mm]
y_7' =& y_8, & y_7(0) &= 0, \\[2mm]
y_8' =& \frac{1}{\phi_1{}^2}\left(\phi_1\left(A\left(y_7 + \frac{\eta}{2}y_8\right) - y_1 y_8 - y_3 y_6 + 2 y_2 y_7 + \frac{M}{1+m^2}(y_7 + my_9) \right) \right. \\
& \left. + \left(A\left(y_2 + \frac{\eta}{2}y_3\right) - y_1 y_3 + y_2^2 + \frac{M}{1+m^2}(y_2 + my_4) \right) 3(n-1)We y_3 y_8 \right), \\[2mm]
& & y_8(0) &= 1, \\[2mm]
y_9' =& y_{10}, & y_9(0) &= 0, \\[2mm]
y_{10}' =& \frac{1}{\phi_2{}^2}\left(\phi_2\left(A\left(y_9 + \frac{\eta}{2}y_{10}\right) + y_4 y_7 + y_2 y_9 - y_1 y_{10} - y_5 y_6 - \frac{M}{1+m^2}(my_7 - y_9) \right) \right.
\end{aligned}
$$

$$+\left(A\left(y_4+\frac{\eta}{2}y_5\right)+y_4y_2-y_1y_5-\frac{M}{1+m^2}(my_2-y_4)\right)3(n-1)Wey_5y_{10}\right),$$

$$y_{10}(0)=0,$$

$$y'_{11}=y_{12}, \qquad\qquad y_{11}(0)=0,$$

$$y'_{12}=y_{13}, \qquad\qquad y_{12}(0)=0,$$

$$y'_{13}=\frac{1}{\phi_1{}^2}\left(\phi_1\left(A\left(y_{12}+\frac{\eta}{2}y_{13}\right)-y_1y_{13}-y_3y_{11}+2y_2y_{12}+\frac{M}{1+m^2}(y_{12}+my_{14})\right)\right.$$
$$\left.+\left(A\left(y_2+\frac{\eta}{2}y_3\right)-y_1y_3+y_2^2+\frac{M}{1+m^2}(y_2+my_4)\right)3(n-1)Wey_3y_{13}\right),$$

$$y_{14}(0)=0,$$

$$y'_{14}=y_{15}, \qquad\qquad y_{14}(0)=0,$$

$$y'_{15}=\frac{1}{\phi_2{}^2}\left(\phi_2\left(A\left(y_{14}+\frac{\eta}{2}y_{15}\right)+y_4y_{12}+y_2y_{14}-y_1y_{15}-y_5y_{11}\right.\right.$$
$$\left.-\frac{M}{1+m^2}(my_{12}-y_{14})\right)+\left(A\left(y_4+\frac{\eta}{2}y_5\right)+y_4y_2-y_1y_5\right.$$
$$\left.\left.-\frac{M}{1+m^2}(my_2-y_4)\right)3(n-1)Wey_5y_{10}\right), \qquad y_{15}(0)=1.$$

The above IVP will be solved numerically by the RK-4 method. To get the approximate solution, the domain of the problem has been taken as $[0,\eta_\infty]$ instead of $[0,\infty)$, where η_∞ is an appropriate finite positive real number. In the above system of equations, the missing conditions ξ_1 and ξ_2, are to be chosen such that

$$y_2(\eta_\infty,\xi_1,\xi_2)=0,\quad y_4(\eta_\infty,\xi_1,\xi_2)=0. \tag{4.27}$$

For the improvement of the missing condition, Newton's method has been implemented which is conducted by the following iterative scheme:

$$\begin{pmatrix}\xi_1^{(k+1)}\\\xi_2^{(k+1)}\end{pmatrix}=\begin{pmatrix}\xi_1^{(k)}\\\xi_2^{(k)}\end{pmatrix}-\left[\begin{pmatrix}y_7 & y_9\\y_{11} & y_{14}\end{pmatrix}^{-1}\begin{pmatrix}y_2^{(k)}\\y_4^{(k)}\end{pmatrix}\right]_{\left(\xi_1^{(k)},\xi_2^{(k)},\eta_\infty\right)} \tag{4.28}$$

The following steps are involved for the accomplishment of the shooting method.

(i) Choice of the guesses $\xi_1=\xi_1{}^{(0)}$ and $\xi_2=\xi_2{}^{(0)}$.

(ii) Choice of a positive small number ϵ.

If $max\{|y_2(\eta_\infty-0)|,|y_4(\eta_\infty-0)|\}<\epsilon$, stop the process otherwise go to (iii).

(iii) Compute $\xi_1^{(k+1)}$ and $\xi_2^{(k+1)}$, $k = 0, 1, 2, 3....$ by using (4.28).

(iv) Repeat (i) and (ii).

In a similar manner, the ODE (4.19) along with the associated BCs can be solved by considering f as a known function.

4.4   Representation of Graphs and Tables

A thorough discussion on the graphs and tables has been conducted which contains the effects of non dimensional parameters on the skin friction coefficient, Nusselt number, velocity behavior and the temperature profile. Table 4.1, explains the impact of magnetic parameter M, Hall current m, unsteadiness A, Weissenberg number W_e and power law-index n on the skin friction coefficients $-C_{fx}Re^{\frac{1}{2}}$ and $C_{fz}Re^{\frac{1}{2}}$. The value $n = 3$ is fixed throughout the discussion. Further, the rising values of M, the skin friction coefficients rises in both directions. Due to rising values of Hall current m, the $-C_{fx}Re^{\frac{1}{2}}$ is reduce while, $C_{fz}Re^{\frac{1}{2}}$ is increases. By ascending values of unsteadiness A, there is a marginal increase in skin friction coefficient along the both directions x and z. Meanwhile, due to extending the values of Wiessinberg number, the skin friction coefficient along x direction is increased and a marginal increment along z direction is seen.

M	m	A	W_e	$-C_{fx}Re^{\frac{1}{2}}$	$C_{fz}Re^{\frac{1}{2}}$
0.5	0.1	0.1	0.05	1.27682813	0.02280321
1				1.47275246	0.03841592
1.13				1.52006638	0.04188206
	0.5			1.24036080	0.09561976
	1			1.17768745	0.12810130
		0.2		1.30688119	0.02219995
		0.3		1.33663405	0.02161821
			0.1	1.29858276	0.02300580
			0.15	1.31813375	0.02318507

TABLE 4.1: Values of the $-C_{fx}Re^{\frac{1}{2}}$ and $-C_{fz}Re^{\frac{1}{2}}$ for different parameters

In Table 4.2, the effects of the significant parameters on Nusselt number $Nu_xRe^{-\frac{1}{2}}$ have been discussed. The rising pattern is found in the $Nu_xRe^{-\frac{1}{2}}$ due to extending

values of Hall Current m, Prandtl number P_r and temperature ratio tr, while the Nusselt number decreases due to accelerating values of magnetic parameter M, unsteadiness parameter A and radiation parameter N_r.

M	m	A	Nr	tr	W_e	Pr	$Nu_xRe^{-\frac{1}{2}}$
0.5	0.1	0.1	2	1	0.05	10	2.71034759
1							2.64150549
1.13							2.62506716
	0.5						2.72241537
	1						2.74397741
		0.2					2.70211916
		0.3					2.69394188
			4				2.47075201
			6				2.38156287
				2			3.92330151
				3			5.21466741
					0.1		2.72299927
					0.15		2.73378326
						15	3.92330151
						20	4.03600482

TABLE 4.2: Values of the $Nu_xRe^{-\frac{1}{2}}$ for different parameters.

The impact of magnetic field parameter M, on the velocity behavior and temperature profile has been discussed in Figures 4.2-4.4 respectively. The ascending values of the M is kept constant, the velocity along the x axis it is decreases and the velocity behavior along the z axis it is increases, while the temperature is also increased gradually. Furthermore, the effects of m Hall current, on the velocity and temperature are depicted in Figures 4.5-4.7. In these figures for the same rising values of m, the velocity profile along the x direction it is increases and a marginal increment found in velocity profile along the z direction and there is a marginal decrease in temperature profile. The effects of Hall current is found when the stability of the magnetic field is too much strong, and the magnetohydrodynamics flow of electrically conducting fluids produce Hall current. Figures 4.8-4.10 show the effects of unsteadiness A on the velocity and temperature profiles. There is a marginal increment in velocity along the x direction due to ascending values of A which is shown in Figure 4.8. Meanwhile, the velocity behavior along z direction reduce, due to rising values of unsteadiness A which is illustrated in Figure

4.9 and the temperature behavior is increase due to the ascending values of the unsteadiness A which is presented in Figure 4.10. Figures 4.11-4.13 display the impacts of Weissenberg number W_e on velocity and the temperature. It is clear from Figures 4.11-4.12 the increasing values of W_e, a marginal decrement is found in the velocity profiles. Furthermore a marginal increment is found in the temperature profile which is given in Figure 4.13. Actually, the Weissenberg number is rises due to presence of time constant Γ and decreases due to presence of viscosity, so higher values of Weissenberg number W_e increase the thermal boundary layer.

Figures 4.14-4.16 show the impact of radiation parameter N_r, Prandtl number P_r and temperature ratio tr on the temperature profile $\theta(\eta)$. The ascending values of the radiation parameter N_r and Prandtl number P_r decrease the temperature behavior within the boundary layer region which is shown in Figure 4.14-4.15. Furthermore the temperature is inversely proportional to the radiation and the Prandtl number is directly proportional to viscous diffusivity and inversely proportion to the thermal diffusivity. The increasing values of temperature ratio tr, the temperature profile shows a growing behavior which is given in Figure 4.16.
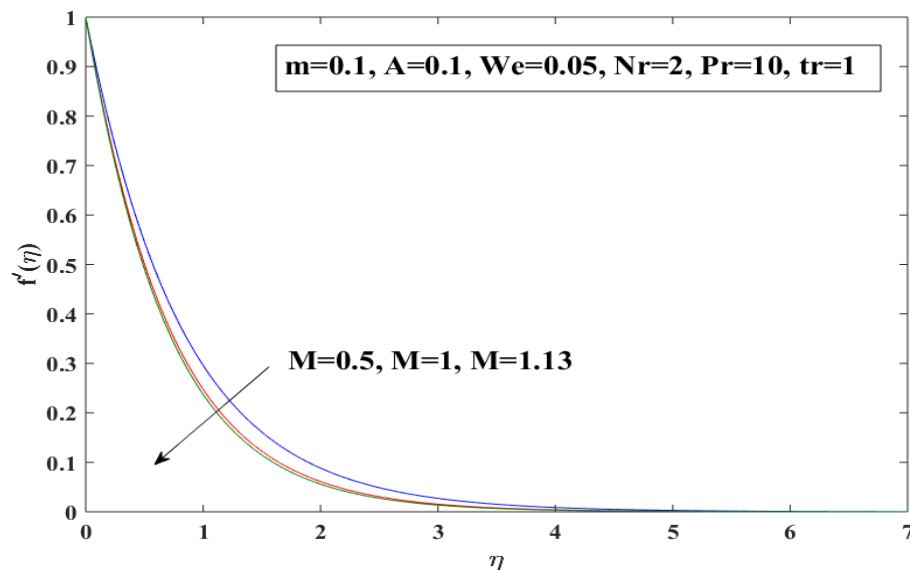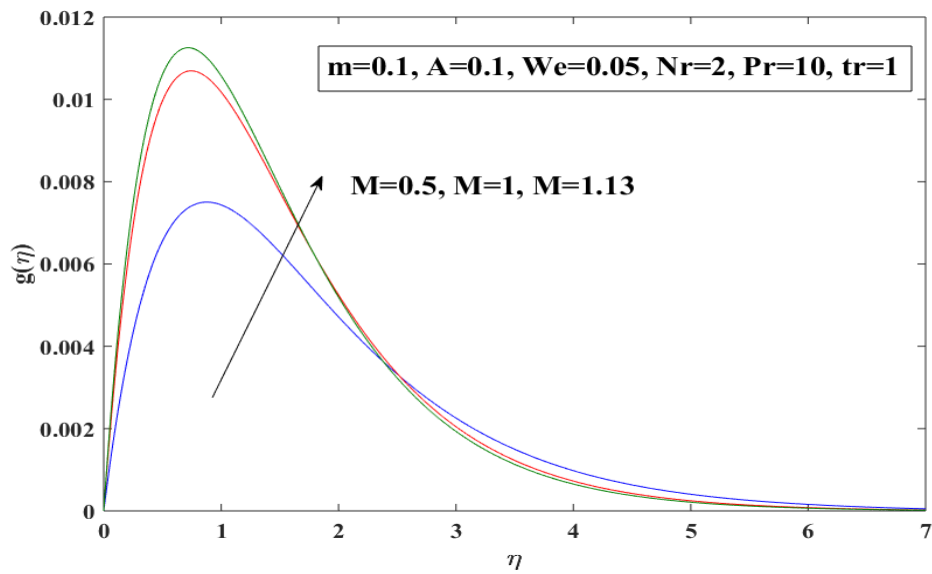

FIGURE 4.2: Variation in $f'(\eta)$

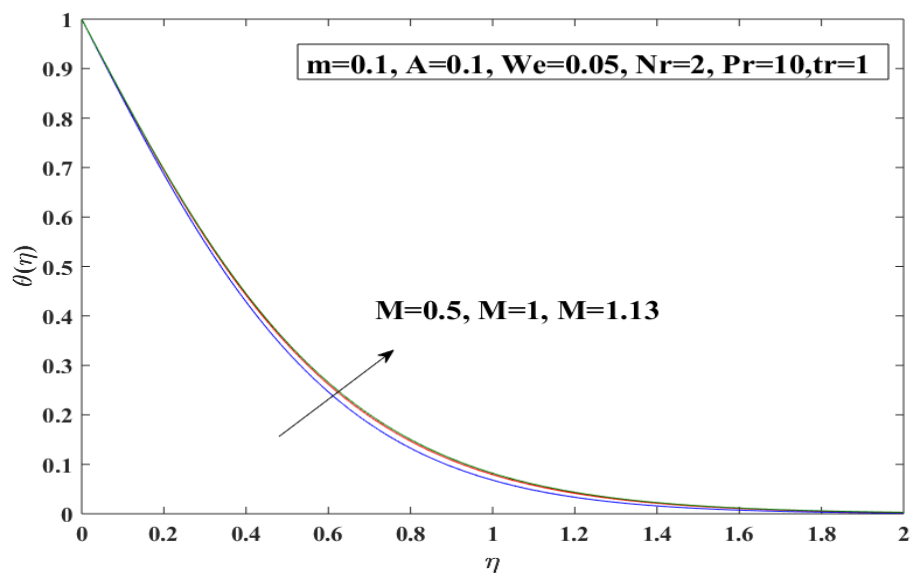FIGURE 4.3: Variation in $g(\eta)$

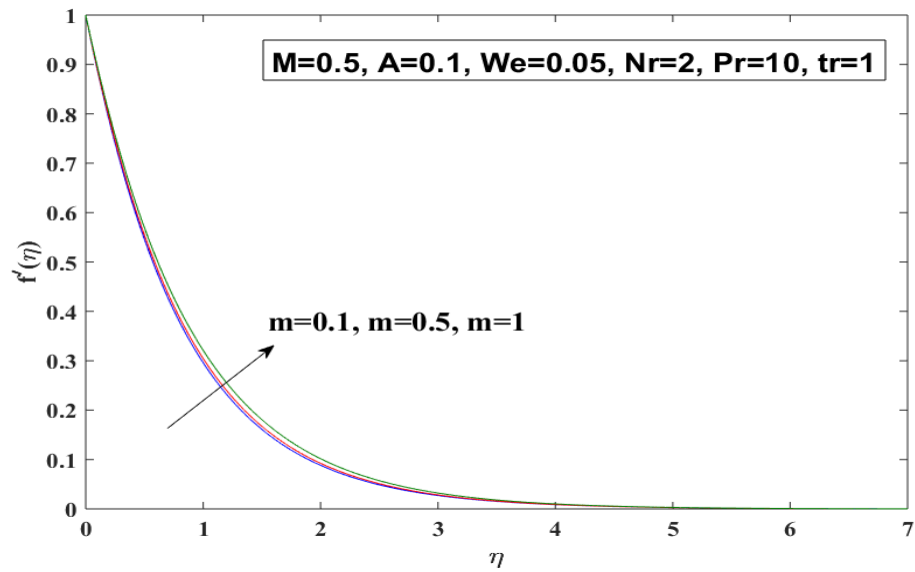FIGURE 4.4: Variation in temperature behavior $\theta(\eta)$

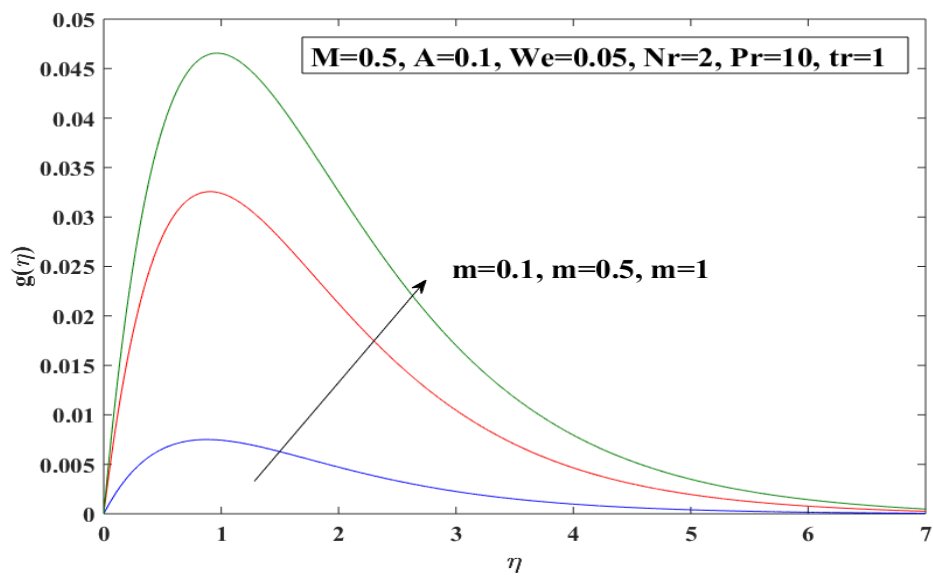FIGURE 4.5: Variation in velocity behavior $f'(\eta)$

FIGURE 4.6: Variation in velocity behavior $g(\eta)$
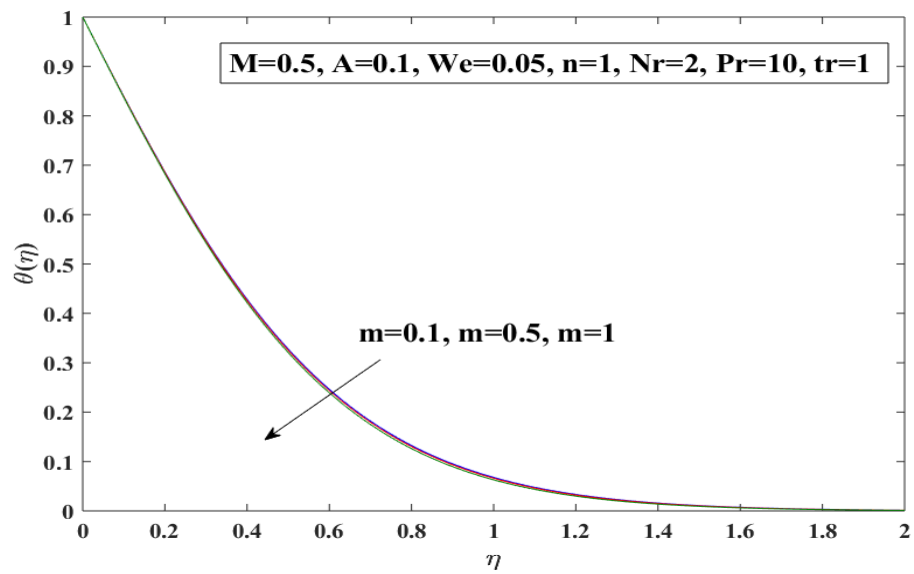
FIGURE 4.7: Variation in temperature behavior $\theta(\eta)$
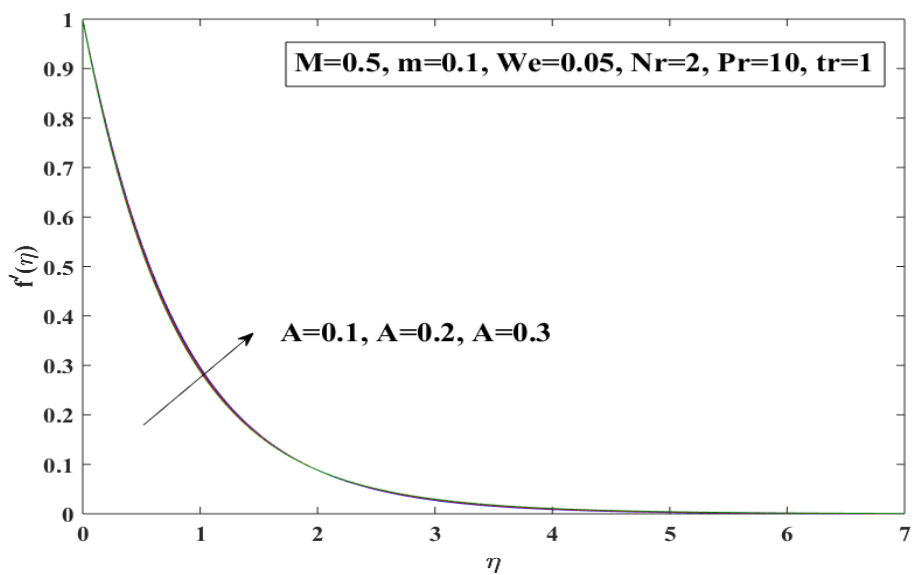

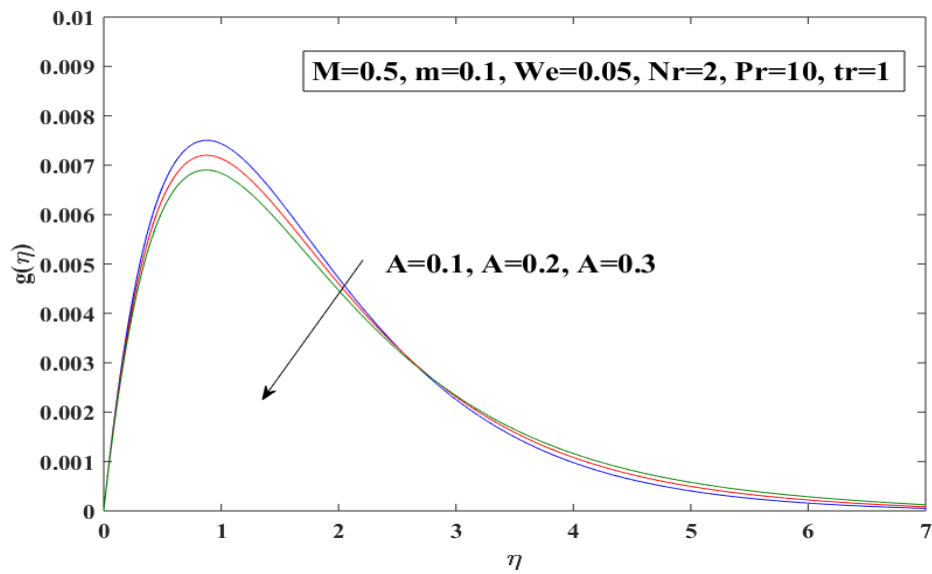FIGURE 4.8: Variation in velocity behavior $f'(\eta)$

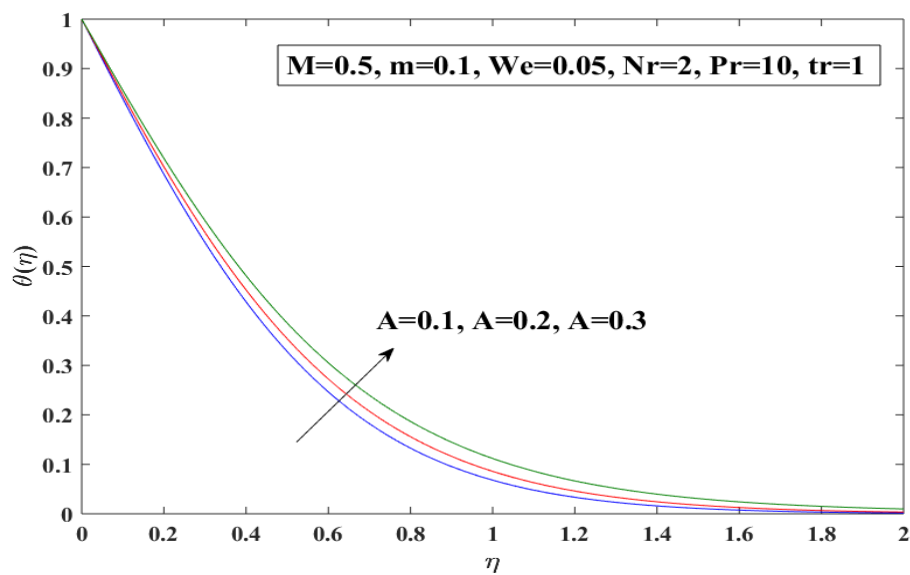FIGURE 4.9: Variation in velocity behavior $g(\eta)$

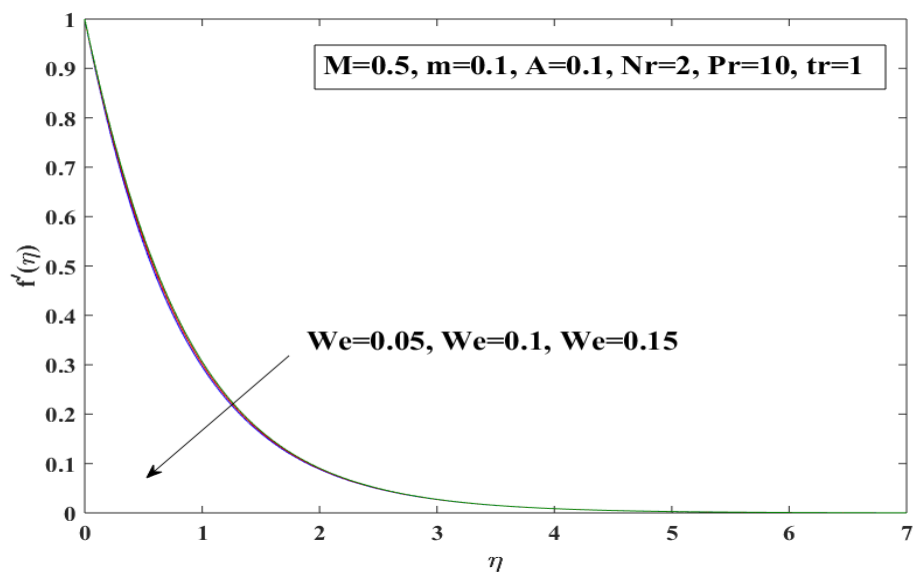FIGURE 4.10: Variation in temperature behavior $\theta(\eta)$

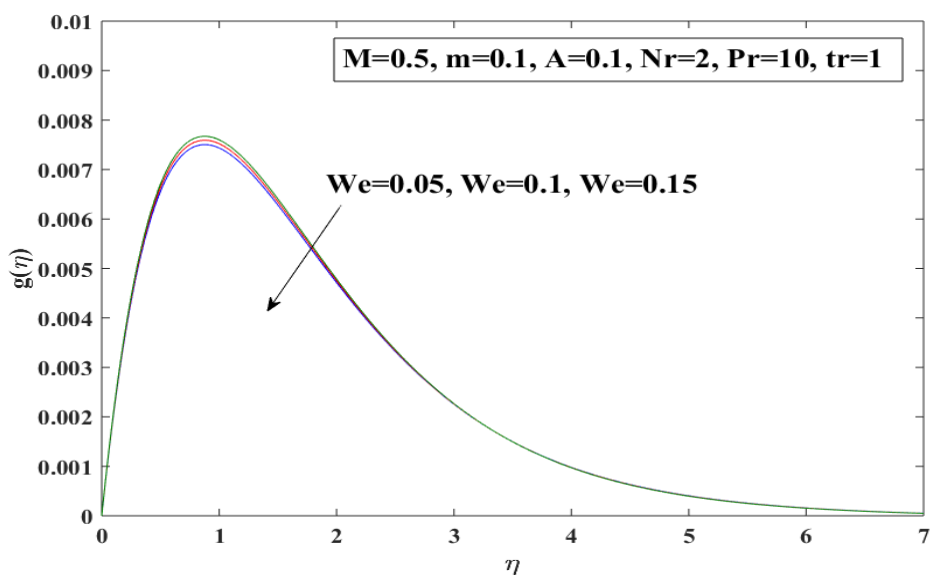FIGURE 4.11: Variation in velocity behavior $f'(\eta)$

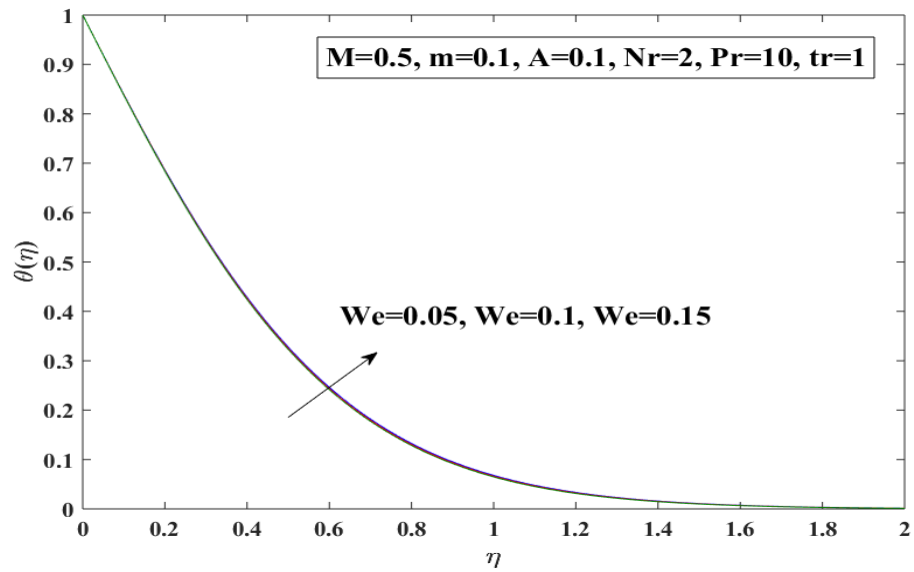FIGURE 4.12: Variation in velocity behavior $g(\eta)$

FIGURE 4.13: Variation in temperature behavior $\theta(\eta)$
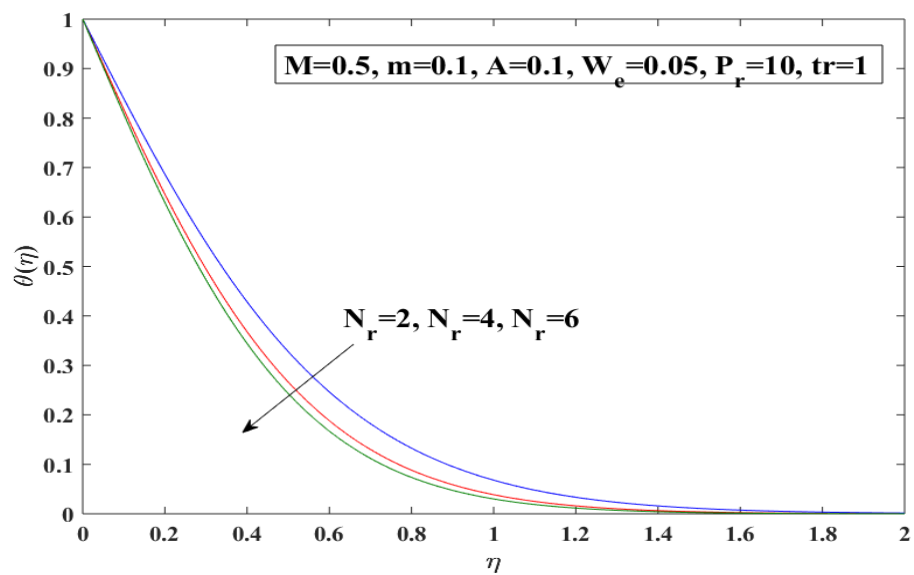

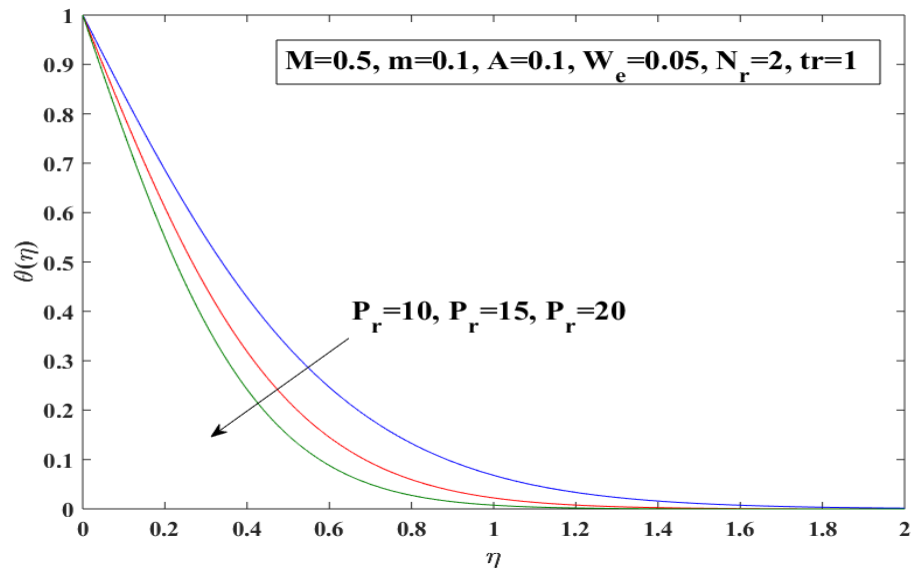FIGURE 4.14: Variation in temperature behavior $\theta(\eta)$

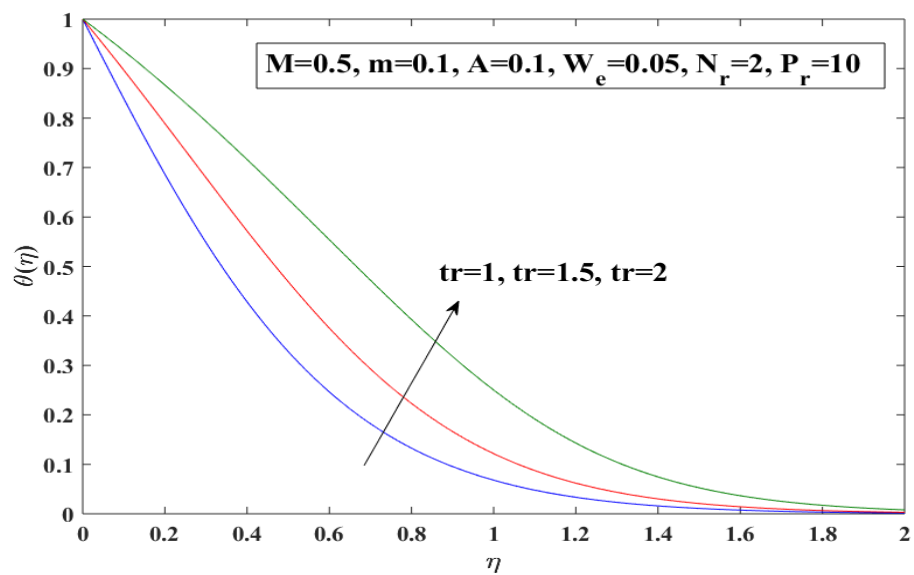FIGURE 4.15: Variation in temperature behavior $\theta(\eta)$

FIGURE 4.16: Variation in temperature behavior $\theta(\eta)$

Chapter 5

Conclusion

Summary of this research work represents the unsteady 3D megnetohydrodynamics flow of Casson and Carreau fluid along a elastically stretchable surface with the Hall current and radiation impacts. Furthermore the impacts of the Weissenberg number and the power-law index have also been discussed. The obtained mathematical model contains the nonlinear PDEs of continuity equation, momentum and heat energy. Furthermore these PDEs are converted into a system of nonlinear ODES by applying the similarity transformations. Meanwhile for the numerical results of ODEs, shooting technique has been utilized. The dimensionless velocity behavior, temperature distribution, skin friction coefficient and Nusselt number have been analyzed for various physical parameters. The numerical results are explained through different figures and tables. Some interesting findings have been listed below.

- Due to the rising values of the magnetic parameter M, the velocity behavior decreases along x axis in both the Casson and Carreau fluids.

- Due to the ascending values of the M magnetic parameter, the velocity behavior increases along z direction in the Carreau fluid.

- Due to the ascending values of the magnetic parameter M, the temperature behavior also increases in both the Carreau and Casson fluids.

- Due to the accelerating values of Hall current m, the velocity rise in z axis and marginal increment found in x direction. While the marginal decrement found in the temperature profile in both the Casson and Carreau fluids.

- A decrement is observed in the velocity behavior due to the rising values of the unsteadiness A. However, no significant change is prominent in the velocity profile along x direction in both the Casson and Carreau fluid.

- An increment is observed in the temperature behavior due to the rising values of the unsteadiness A in both the Casson and Carreau fluids.

- In the presence of the magnetic parameter M, the $-C_{fx}Re^{\frac{1}{2}}$ and $C_{fz}Re^{\frac{1}{2}}$, increases in both the Casson and Carreau fluids.

- A decrement is noticed in the $-C_{fx}Re^{\frac{1}{2}}$ by increasing values of Hall current m, in the Casson fluid.

- The effects of Weissenberg number W_e on the velocity and temperature are not so prominent. However a marginal decrement in the velocity and marginal increment in temperature are observed.

Bibliography

[1] L. J. Crane, "Flow past a stretching plate," *Zeitschrift für angewandte Mathematik und Physik ZAMP*, vol. 21, no. 4, pp. 645–647, 1970.

[2] E. M. Elbashbeshy, "Heat transfer over a stretching surface with variable surface heat flux," *Journal of Physics D: Applied Physics*, vol. 31, no. 16, p. 1951, 1998.

[3] T. R. Mahapatra and A. Gupta, "Heat transfer in stagnation-point flow towards a stretching sheet," *Heat and Mass transfer*, vol. 38, no. 6, pp. 517–521, 2002.

[4] M. Z. Salleh, R. Nazar, and I. Pop, "Boundary layer flow and heat transfer over a stretching sheet with Newtonian heating," *Journal of the Taiwan Institute of Chemical Engineers*, vol. 41, no. 6, pp. 651–655, 2010.

[5] M. Misra, N. Ahmad, and Z. U. Siddiqui, "Unsteady boundary layer flow past a stretching plate and heat transfer with variable thermal conductivity," *World Journal of Mechanics*, vol. 2, no. 01, p. 35, 2012.

[6] K. Pavlov, "Magnetohydrodynamic flow of an incompressible viscous fluid caused by deformation of a plane surface," *Magnitnaya Gidrodinamika*, vol. 4, no. 1, pp. 146–147, 1974.

[7] H. Alfvén, "Existence of electromagnetic-hydrodynamic waves," *Nature*, vol. 150, no. 3805, p. 405, 1942.

[8] T. Sarpkaya, "Flow of non-Newtonian fluids in a magnetic field," *AIChE Journal*, vol. 7, no. 2, pp. 324–328, 1961.

[9] C. Wang, "Liquid film on an unsteady stretching surface," *Quarterly Journal of Applied Mathematics*, vol. 48, no. 4, pp. 601–610, 1990.

[10] H. Takhar, A. Chamkha, and G. Nath, "Unsteady flow and heat transfer on a semi-infinite flat plate with an aligned magnetic field," *International Journal of Engineering Science*, vol. 37, no. 13, pp. 1723–1736, 1999.

[11] A. J. Chamkha and A. Al-Mudhaf, "Unsteady heat and mass transfer from a rotating vertical cone with a magnetic field and heat generation or absorption effects," *International journal of thermal sciences*, vol. 44, no. 3, pp. 267–276, 2005.

[12] A. J. Chamkha and S. Ahmed, "Similarity solution for unsteady MHD flow near a stagnation point of a three-dimensional porous body with heat and mass transfer, heat generation/absorption and chemical reaction," *Journal of Applied Fluid Mechanics*, vol. 4, no. 2, pp. 87–94, 2011.

[13] A. Ishak, R. Nazar, and I. Pop, "Boundary layer flow and heat transfer over an unsteady stretching vertical surface," *Meccanica*, vol. 44, no. 4, pp. 369–375, 2009.

[14] M. A. El-Aziz, "Flow and heat transfer over an unsteady stretching surface with Hall effect," *Meccanica*, vol. 45, no. 1, pp. 97–109, 2010.

[15] A. J. Chamkha, "Coupled heat and mass transfer by natural convection about a truncated cone in the presence of magnetic field and radiation effects," *Numerical Heat Transfer: Part A: Applications*, vol. 39, no. 5, pp. 511–530, 2001.

[16] M. A. El-Aziz, "Radiation effect on the flow and heat transfer over an unsteady stretching sheet," *International Communications in Heat and Mass Transfer*, vol. 36, no. 5, pp. 521–524, 2009.

[17] M. Rashidi and S. Abbasbandy, "Analytic approximate solutions for heat transfer of a micropolar fluid through a porous medium with radiation," *Communications in Nonlinear Science and Numerical Simulation*, vol. 16, no. 4, pp. 1874–1889, 2011.

[18] D. Pal, "Hall current and MHD effects on heat transfer over an unsteady stretching permeable surface with thermal radiation," *Computers & Mathematics with Applications*, vol. 66, no. 7, pp. 1161–1180, 2013.

[19] N. Casson, "A flow equation for pigment-oil suspensions of the printing ink type," *Rheology of Disperse Systems*, pp. 84–104, 1959.

[20] R. Dash, K. Mehta, and G. Jayaraman, "Casson fluid flow in a pipe filled with a homogeneous porous medium," *International Journal of Engineering Science*, vol. 34, no. 10, pp. 1145–1156, 1996.

[21] N. Eldabe, G. Saddeck, and A. El-Sayed, "Heat transfer of MHD non-Newtonian Casson fluid flow between two rotating cylinders," *Mechanics and Mechanical Engineering*, vol. 5, no. 2, pp. 237–251, 2001.

[22] S. Nadeem, R. U. Haq, N. S. Akbar, and Z. H. Khan, "MHD three-dimensional Casson fluid flow past a porous linearly stretching sheet," *Alexandria Engineering Journal*, vol. 52, no. 4, pp. 577–582, 2013.

[23] S. Pramanik, "Casson fluid flow and heat transfer past an exponentially porous stretching surface in presence of thermal radiation," *Ain Shams Engineering Journal*, vol. 5, no. 1, pp. 205–212, 2014.

[24] G. Mahanta and S. Shaw, "3D Casson fluid flow past a porous linearly stretching sheet with convective boundary condition," *Alexandria Engineering Journal*, vol. 54, no. 3, pp. 653–659, 2015.

[25] M. B. Ashraf, T. Hayat, and A. Alsaedi, "Mixed convection flow of Casson fluid over a stretching sheet with convective boundary conditions and Hall effect," *Boundary Value Problems*, vol. 2017, no. 1, p. 137, 2017.

[26] A. Butt, M. Tufail, and A. Ali, "Three-dimensional flow of a magnetohydrody-namic Casson fluid over an unsteady stretching sheet embedded into a porous medium," *Journal of Applied Mechanics and Technical Physics*, vol. 57, no. 2, pp. 283–292, 2016.

[27] M. I. Khan, M. Waqas, T. Hayat, and A. Alsaedi, "A comparative study of Casson fluid with homogeneous-heterogeneous reactions," *Journal of Colloid and Interface Science*, vol. 498, pp. 85–90, 2017.

[28] N. S. Akbar and Z. H. Khan, "Metachronal beating of cilia under the influence of Casson fluid and magnetic field," *Journal of Magnetism and Magnetic Materials*, vol. 378, pp. 320–326, 2015.

[29] N. S. Akbar, "Influence of magnetic field on peristaltic flow of a Casson fluid in an asymmetric channel: application in crude oil refinement," *Journal of Magnetism and Magnetic Materials*, vol. 378, pp. 463–468, 2015.

[30] A. Khalid, I. Khan, A. Khan, and S. Shafie, "Unsteady MHD free convection flow of Casson fluid past over an oscillating vertical plate embedded in a porous medium," *Engineering Science and Technology, an International Journal*, vol. 18, no. 3, pp. 309–317, 2015.

[31] S. A. Shehzad, T. Hayat, and A. Alsaedi, "Three-Dimensional MHD Flow of Casson Fluid in Porous Medium with Heat Generation." *Journal of Applied Fluid Mechanics*, vol. 9, no. 1, 2016.

[32] K. A. Maleque, "MHD Non-Newtonian Casson fluid heat and mass transfer flow with exothermic/endothermic binary chemical reaction and activation energy," *American Journal of Heat and Mass Transfer*, vol. 3, no. 1, pp. 166–185, 2016.

[33] H. Kataria and H. Patel, "Heat and mass transfer in magnetohydrodynamic (MHD) Casson fluid flow past over an oscillating vertical plate embedded in porous medium with ramped wall temperature," *Propulsion and Power Research*, vol. 7, no. 3, pp. 257–267, 2018.

[34] R. Vijayaragavan and S. Karthikeyan, "Hall Current Effect on Chemically Reacting MHD Casson Fluid Flow with Dufour Effect and Thermal Radiation." *Open Access Quarterly International Journal*, vol. 2, pp. 228–245, 2018.

[35] R. Nandkeolyar, "A numerical treatment of unsteady three-dimensional hydromagnetic flow of a Casson fluid with Hall and radiation effects," *Results in Physics*, vol. 11, pp. 966–974, 2018.

[36] T. Hayat, S. Asad, M. Mustafa, and A. Alsaedi, "Boundary layer flow of Carreau fluid over a convectively heated stretching sheet," *Applied Mathematics and Computation*, vol. 246, pp. 12–22, 2014.

[37] M. Khan and M. Azam, "Unsteady boundary layer flow of Carreau fluid over a permeable stretching surface," *Results in Physics*, vol. 6, pp. 1168–1174, 2016.

[38] T. Hayat, I. Ullah, B. Ahmad, and A. Alsaedi, "Radiative flow of Carreau liquid in presence of Newtonian heating and chemical reaction," *Results in Physics*, vol. 7, pp. 715–722, 2017.

[39] M. Khan, M. Malik, T. Salahuddin, and I. Khan, "Numerical modeling of Carreau fluid due to variable thicked surface," *Results in physics*, vol. 7, pp. 2384–2390, 2017.

[40] J. H. Ferziger and M. Peric, *Computational Methods for Fluid Dynamics*. Springer Science & Business Media, pp. 1, 2012.

[41] Y. Cencel and J. Cimbala, *Fluid Mechanics, Fundamentals and Applications*. McGraw-Hill Internat. Ed., pp. 1–15, 2006.

[42] D. J. Tritton, *Physical Fluid Dynamics*. Springer Science & Business Media, pp. 1, 2012.

[43] F. M. White, *Fluid Mechanics*. McGraw-Hill, New York, pp. 25, 2003.

[44] R. Bansal, *A Textbook of Fluid Mechanics and Hydraulic Machines*. Laxmi Publications, pp. 1–7, 2004.

[45] S. S. Molokov, R. Moreau, and H. K. Moffatt, *Magnetohydrodynamics: Historical evolution and trends.* Springer Science & Business Media, pp. 441, 2007, vol. 80.

[46] T. Papanastasiou, G. Georgiou, and A. N. Alexandrou, *Viscous Fluid Flow.* CRC press, pp. 456, 1999.

[47] F. M. White and I. Corfield, *Viscous Fluid Flow.* McGraw-Hill New York, pp. 60–75, 2006, vol. 3.

[48] J. Kunes, *Dimensionless Physical Quantities in Science and Engineering.* Elsevier, pp. 441, 2012.